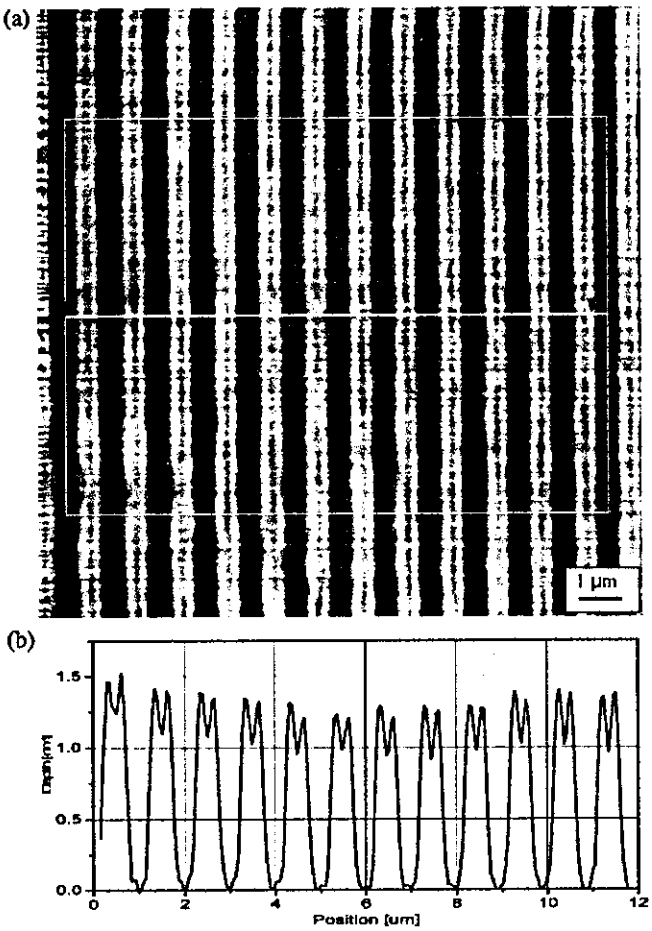

Figure 8. (a) Atomic force microscopy image corresponding to the region in Figure 7; (b) average cross-section profile for the area delimited by the thin white line in panel a.

place in the photoirradiated areas. As seen in Figure 8, photoirradiated regions are recessed from the surrounding unirradiated regions. Recessed depths determined from cross sections of the AFM images were 1.4 ± 0.1 nm. These depths were smaller than ellipsometry-measured SAMs thicknesses, i.e., 1.68–1.7 nm. That is because a thin layer of SiO_x remains on the substrate even when all organic parts are removed.[29] The thickness of the remaining SiO_x layer was estimated by ellipsometry to be ca. 0.2 nm. Therefore, ODS SAMs were concluded to be photodecomposed and removed in the photoirradiated regions.

Conclusions

Using a molecular fluorine laser at 157 nm wavelength, submicron patterning of organosilane SAMs was successfully demonstrated on the basis of photolithography. An organosilane, namely, ODS, was chosen to create by chemisorption a SAM onto an oxide-covered Si substrate, which SAM was subsequently patterned using the laser. After an initial air evacuation, the optical path of the laser beam and the photomask–sample space were backfilled and then purged with nitrogen. The photoirradiation process and the resulting pattern were investigated using XPS, SPM, ellipsometry, and contact angle measurements. The acquired SPM images show that 500 nm size features can be successfully photoprinted in this way.

Potential applications can be identified in the field of electronic devices, organic templates, and so forth. These promising initial results will be further investigated to check the validity of the approach, to quantify the necessary laser fluence for optimal photoirradiation of the SAM, and to identify possible bottlenecks such as, for instance, contamination problems resulting from the long-term exposure of the optical path to various organic compounds.

Acknowledgment. This study was partially supported by the Aichi Science and Technology Foundation.

LA0480944

(29) Brunner, H.; Vallant, T.; Mayer, U.; Hoffmann, H. *Langmuir* **1996**, *12*, 4614–4617.

Langmuir 2004, *20*, 5182–5184

Generation of Amino-Terminated Surfaces by Chemical Lithography Using Atomic Force Microscopy

N. Saito,*,† N. Maeda,† H. Sugimura,† and O. Takai‡

Department of Materials Engineering, Graduate School of Engineering, Nagoya University, Furo-cho, Chikusa-ku, Nagoya 464-8603, Japan, and Center for Integrated Research in Science and Engineering, Nagoya University, Furo-cho, Chikusa, Nagoya 464-8603, Japan

Received July 23, 2003. In Final Form: January 30, 2004

Self-assembled monolayers (SAMs) covered with nitroso end groups were reduced using an atomic force microscope. As the bias voltage become more negative (beyond −4 V), the surface potential of the scanned area become closer to that of the amino-terminated SAM. Following this chemical change, however, no change in topographic features was detected, implying retained stability of the underlying SAM layer. We then released carboxylate-modified polystyrene (PS) spheres into a pH 4 solution containing the sample. Subsequent imaging with atomic force microscopy (AFM) revealed that these PS spheres were only selectively immobilized on the regions that were originally scanned at −6 V to form amino termination. In summary, using AFM set to a specific voltage, we were able to selectively generate micropatterned regions of the SAM with amino termination.

Introduction

Amino-terminated self-assembled monolayers (SAMs) on silicon substrate have a potential as templates for biosensor or molecular devices. Since amino groups are able to link with target molecules such as deoxyribonucleic acid (DNA) and antibody-forming cell, many researchers had investigated amino-terminated SAMs.[1-5] To fabricate components of future microdevices, such templates might offer high chemical reactivity which is restricted to specific microregions. Thus, the amino-terminated regions must be prepared on given points of a substrate.

Such a microstructure can be accomplished by maskless lithography techniques such as focus ion beam and electron beam lithography techniques.[6-10] However, these lithography techniques cause radiation damage to the amino-terminated surface of a SAM due to the excessive energy applied. To overcome these problems, we developed a soft chemical lithography process for the generation of amino-terminated surface, that is, a technique which would convert only the functional groups. Scanning probe lithography (SPL) is based on an electrochemical approach and can be employed to realize such a soft process by controlling the applied potential.[11,12] SPL had been applied in many cases, however, for the elimination of SAMs.

In our present research, we have attempted through chemical lithography to use an atomic force microscope to produce amino-terminated regions on a sample surface without damage to the molecule. To realize this, we focused out attention on the reactivity of the amino-terminated surface, as described below. The amino-terminated surface is first oxidized by heating in air. Following this, a positive potential is electrochemically applied beyond the oxidation–reduction (OR) potential. The nitroso- or nitro-terminated surface can be converted back into an amino-terminated surface by applying electrochemical negative potential below the OR potential.

In this investigation, an amino-terminated SAM was prepared from (*p*-aminophenyl)trimethoxysilane (APhS) though chemical vapor deposition (CVD). The root mean square (rms) of APhS-SAM was 0.32 nm, which was approximately equal to the rms of silicon wafer. This was then first oxidized by heating in air. Next, the oxidized surface was then converted into an amino-terminated surface by chemical lithography. The functional groups on the surfaces thus obtained by chemical lithography were confirmed by selectively labeling the carboxyl-terminated latex particles in order to detect the amino groups.

Experimental Section

The APhS-SAMs were prepared on the substrates of n-type silicon by CVD.[13] A silicon surface covered with a thin oxide layer (ca. 2 nm) was hydroxylated and cleaned simultaneously by a UV/ozone cleaning method. The substrates were then heated together with a container of APhS in an oven, thus depositing APhS-SAMs when the precursor reacted with the hydroxyls on the substrate surfaces. The reaction temperature was 373 K, and the reaction time was 1 h.

Chemical lithography was conducted with an atomic force microscope (Seiko Instruments Inc., SPA-300HV + SPI-3800N) in air. The force constant of gold-coated silicon cantilever was

† Department of Materials Engineering, Graduate School of Engineering, Nagoya University.

‡ Center for Integrated Research in Science and Engineering, Nagoya University.

(1) Petri, D. F. S.; Wenz, G.; Schunk, P.; Schimmel, T. *Langmuir* **1997**, *15*, 4520–4523.

(2) Yang, Z.; Frey, W.; Oliver, T.; Chilkoti, A. *Langmuir* **2000**, *16*, 1751–1758.

(3) Turyan, I.; Matsue, T.; Mandler, D. *Anal. Chem.* **2000**, *72*, 3431–3435.

(4) Geyer, W.; Stadler, V.; Eck, W.; Golzhauser, A.; Grunze, M.; Sauer, M.; Weimann, T.; Hinze, P. *J. Vac. Sci. Technol., B* **2001**, *19*, 2732–2735.

(5) Chirakul, P.; Perez-Luna, V. H.; Owen, H.; Lopez, G. P. *Langmuir* **2002**, *18*, 4234–4330.

(6) Pan, M.; Yun, M.; Kozicki, M. N.; Whidden, T. K. *Superlattices Microstruct.* **1996**, *20*, 369–376.

(7) Ada, E. T.; Hanley, L.; Etchin, S.; Melngailis, J.; Dressick, W. J.; Chen, M. S.; J. M. Calvert, J. M. *J. Vac. Sci. Technol., B* **1995**, *13*, 2189–2196.

(8) Lercel, M. J.; Whelan, C. S.; Craighead, H. G.; Seshadri, K.; Allara, D. L. *J. Vac. Sci. Technol., B* **1996**, *14*, 4085–4090.

(9) Kidoaki, S.; Matsuda, T. *Langmuir* **1999**, *15*, 7639–7646.

(10) Harnett, C. K.; Satyalakshmi, K. M.; Craighead, H. G. *Langmuir* **2001**, *17*, 178–182.

(11) Sugimura, H.; Okiguchi, K.; Nakagiri, N. *Jpn. J. Appl. Phys. 1* **1996**, *35*, 3749–3753.

(12) Xia, Y.; Rogers, J. A.; Paul, K. E.; Whitesides, G. M. *Chem. Rev.* **1999**, *99*, 1823–1848.

(13) Sugimura, H.; Hozumi, A.; Kameyama, T.; Takai, O. *Surf. Interface Anal.* **2002**, *34*, 550–554.

10.1021/la0353428 CCC: $27.50 © 2004 American Chemical Society
Published on Web 05/20/2004

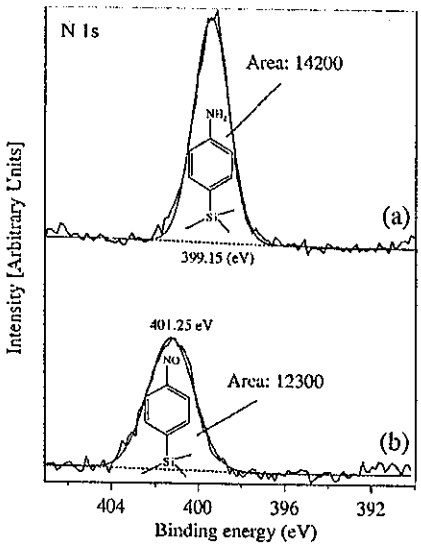

Figure 1. XPS N 1s spectra of APhS-SAM: (a) before and (b) after heat treatment.

0.1 N/m (Seiko Instruments Inc., Micro Cantilever, type SI-AF01-A). Bias voltages of −1 to −6 V were applied (the substrate corresponds to a cathode). The SPL areas are a square 20 μm on a side. After chemical lithography, the sample surfaces were observed in a nitrogen atmosphere with a Kelvin force probe microscope (KPFM) (Seiko Instruments Inc., SPA-300HV+SPI-3800N) using a gold-coated silicon cantilever (Seiko Instruments Inc., Micro Cantilever, type SI-DF3-A). The details of the KPFM measurements were determined on the basis of our previous research.[14] We observed the SPL areas of 20 μm in KPFM and AFM images (150 μm × 150 μm).

Some samples were immersed in a solution dispersed with carboxylate-modified polystyrene fluorescence spheres (CM-FluoSpheres; Molecular Probes, Inc., model F-8888, 0.06% solution in water) for 1 h under mild agitation. After immersion, the samples were rinsed with Mill-Q water and blown dry by N_2 gas stream. Dark-field images of the sample surfaces after immobilization were obtained using an optical microscope (Nikon, ECLIPSE-ME600).

Results and Discussion

The water contact angle of the APhS-SAM became saturated at approximately 60° at the reaction time of 1 h. This value agrees with that obtained in previous reports.[16] Furthermore, the film thickness of 0.6 nm, as determined by ellipsometry, corresponded approximately to the distance from Si to N atoms in the precursor. Figure 1a shows a XPS N 1s spectrum of APhS-SAM. Its peak of 399.1 eV is assigned to the amino group attached to an aromatic ring, as indicated. To clearly demonstrate the presence of the amino group, the APhS-SAM was micropatterned by vacuum ultraviolet lithography, thus dividing the small surface into distinct APhS-SAM and SiO_x regions. The functional groups of the SAM were confirmed by the selective adsorption of carboxylate-modified polystyrene fluorescence spheres in a pH 4 solution.[15] The $-NH_2$ and $-COOH$ groups in the pH 4 solution were converted into $-NH_3^+$ and $-COO^-$ ion groups, so that the selective adsorption of polystyrene spheres on to the substrate proceeded due to their attractive interaction

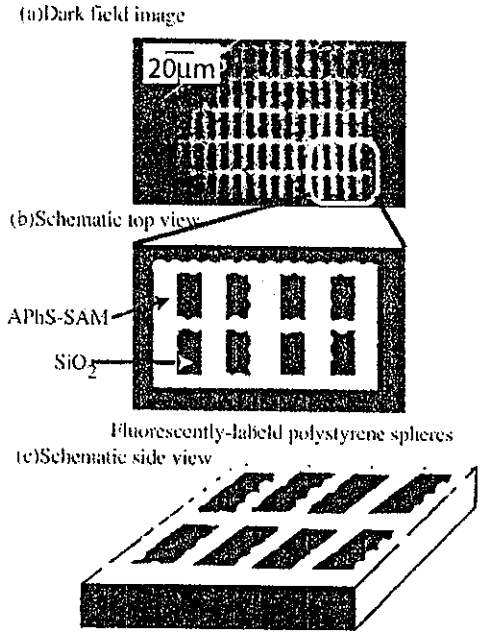

Figure 2. Dark field image of micropatterned APhS-SAM/SiO_2 sample after immersion in a pH 4 solution containing carboxylate-modified polystyrene fluorescence spheres. Top and bottom views indicating the APhS-SAM and SiO_2 regions are also illustrated.

to the surface. Under this pH condition, the regions of silica on the surface were negatively charged and the carboxylate-modified polystyrene fluorescence spheres did not adsorb onto it. Figure 2 shows an image acquired by dark field microscopy of the micropatterned APhS/SiO_2 sample after immersion. The lighter areas between the dark rectangular regions correspond to APhS-SAM. This dark-field image indicates that carboxylate-modified polystyrene fluorescence spheres selectively adsorbed on the APhS-SAM since scattered light due to surface roughness can be observed. From these results, we determined that an APhS-SAM had been successfully prepared.

APhS-SAM samples were heated at 350 °C for 3 h in air in order to convert their amino groups into nitroso groups. Figure 1b shows XPS N 1s spectrum of the sample after the heat treatment. The peak areas of the spectra before and after the heat treatment did not greatly change. The center of peak in the spectrum seen in Figure 1b was located at ca. 401 eV, which is assigned to nitroso groups (−NO). Furthermore, we can confirm that the C 1s spectrum after heat treatment was also identical with the spectrum of APhS-SAM. These results indicate that only amino groups were converted into nitroso groups without decomposition of the aromatic rings and siloxane networks.

A gold-coated probe was scanned on nitroso-terminated SAM in air at bias voltages of −1 to −6 V. Parts a−c of Figure 3 show topographic images, surface potential images, and the surface potential profile, respectively. As seen in Figure 3a, no topographic features were detected in this bias range. On the other hand, the surface potential of the probe-scanned area against the nitroso-terminated surface became more positive as the bias voltages became more negative. In particular, the surface potentials changed drastically at ca. −4 V. The amino- and nitroso-terminated surfaces have positive and negative charges, respectively, based on permanent dipole moments. Consequently, the surface potential of the amino-terminated

(14) Hayashi, K.; Saito, N.; Sugimura, H.; Takai, O.; Nakagiri, N. *Langmuir* **2002**, *18*, 7469−7472.
(15) Hayashi, K.; Sugimura, H.; Takai, O. *Appl. Surf. Sci.* **2002**, *188*, 513−518.
(16) Hozumi, A.; Yokogawa, Y.; Kameyama, T.; Sugimura, H.; Hayashi, K.; Shirayama, H.; Takai, O., *J. Vac. Sci. Technol., B* **2001**, *19*, 1812−1816.

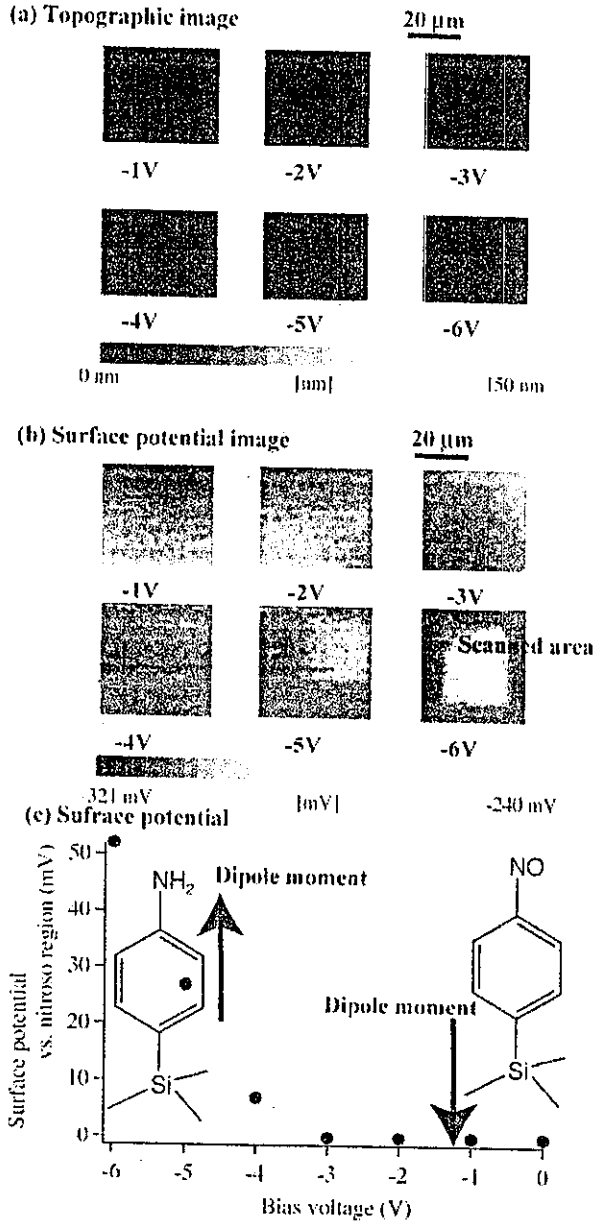

Figure 3. Topographic images (a), surface potential images (b), and surface potential profile (c) of nitroso-terminated SAMs chemically modified using AFM, at different bias voltages.

surface is more positive than that of the nitroso-terminated surface. Interpretation of the images in Figure 3 could be as follows. The change in tip potential has direct correlation with the generation of amino groups in the areas scanned where amino groups were generated. To confirm this, we show that carboxylate-modified polystyrene fluorescence spheres immobilize (in a solution of pH 4) on the SPM scanned areas of the sample. The results are shown in the dark field images of Figure 4. Figure 4 shows

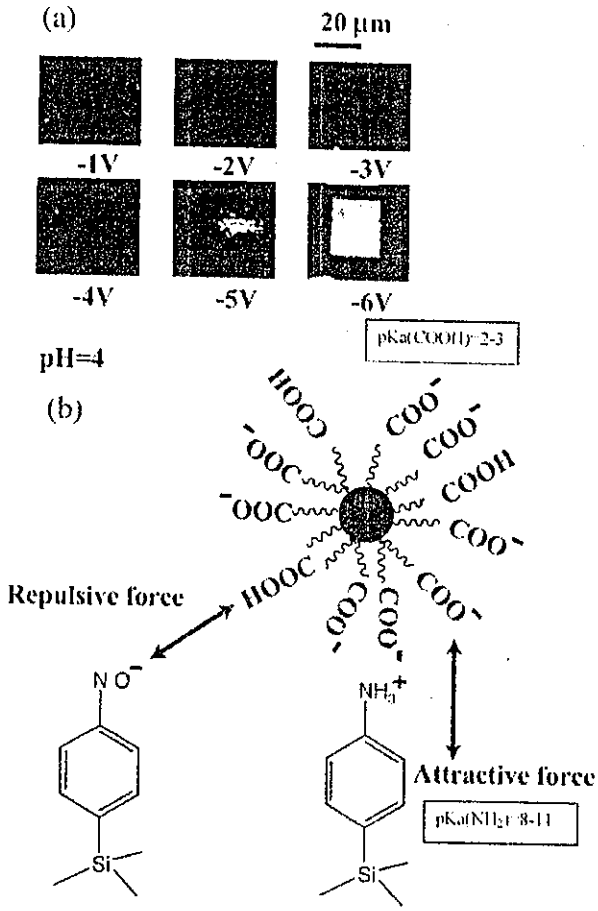

Figure 4. Dark field images of chemically lithographed nitroso-terminated SAMs after immersion in a pH 4 solution containing carboxylate-modified, fluorescently labeled polystyrene spheres.

dark field microscopic images of these samples. The fluorescently labeled polystyrene spheres appear to selectively adsorb in areas that were scanned with a bias of −6. These topographic images correlate well with the surface-potential images of Figure 3b. These results demonstrate that our chemical lithography technique selectively generates the amino groups at desired locations at the micrometer-scale on the sample.

In summary, amino-terminated micrometer-scale regions on silicon substrates surfaces were successfully generated by chemical lithography using atomic force microscopy. This technique may prove useful to fabricate biochips on silicon substrates via a bottom up approach, as demonstrated here.

Acknowledgment. This work has been supported by the "Biomimetic Materials Processing" (No. JSPS-RFTF 99R13101), Research for the Future (RFTF) Program, Japan Society for the Promotion of Science.

LA0353428

Chemoenzymatically Synthesized Glycoconjugate Polymers†

Yoshiko Miura,* Takayasu Ikeda, and Kazukiyo Kobayashi

Department of Molecular Design and Engineering, Graduate School of Engineering, Nagoya University, Furo-cho, Chikusa-ku, Nagoya, Aichi 464-8603, Japan

Received October 29, 2002; Revised Manuscript Received January 5, 2003

Glycoconjugate polymers with poly(vinyl alcohol) (PVA) backbone were synthesized via a chemoenzymatic method. The sugar alcohols of maltose and lactose were submitted to transesterification in the presence of lipases. The esterification was achieved with high selectivity and yield, and the resulting maltitol and lactitol 6-vinyl sebacates were polymerized by a conventional radical initiator with hydrogen peroxide and ascorbic acid. The glycoconjugate polymers carrying α-glucose and β-galactose as recognition signals showed the biological activity such as lectin recognition abilities and hepatocyte adhension. The biodegradability of these polymers was modest but higher than PVA.

Introduction

Carbohydrates on cell surfaces serve as significant biological signals and play important roles in numerous intercellular recognition processes.[1] However, the interactions of isolated carbohydrate ligands with carbohydrate-binding proteins (lectins) are low in affinity and broad in specificity.[2] The carbohydrate signals in biological system are often amplified by the multivalency of carbohydrates or the "glyco-cluster effect".[3] Synthetic glyco-clusters are also reported to amplify the carbohydrate signals similarly to the natural carbohydrate ligands.[4-6] In particular, synthetic glycoconjugate polymers substituted with pendant saccharide have attracted a great attention as synthetic glyco-clusters.[7] We have investigated artificial glycoconjugate polymers with hydrophobic main chains and hydrophilic pendant carbohydrates. These polymers are reported to form characteristic cylindrical conformation in water due to the amphiphilic properties.[8] The densely packed glyco-clusters exhibited unique biological recognition abilities such as lectin recognition, hepatocyte culture, and virus adsorption. In the present paper, we have elaborated a facile synthesis of glycoconjugate polymers applying enzymatic catalysis that is of greater advantage in terms of chemoselectivity and efficiency and also from the aspects of green chemistry (Figure 1).

Esterases such as lipases and proteases have been reported to be powerful catalysts for chemoselective esterification of carbohydrates.[9-11] A variety of sugar-based polymers were synthesized via enzymatic esterification of carbohydrates.[12] As well, polymers of the carbohydrate vinyl esters were reported to indicate the high biodegradability in soil.[13] To the best of our knowledge, however, there has been no paper

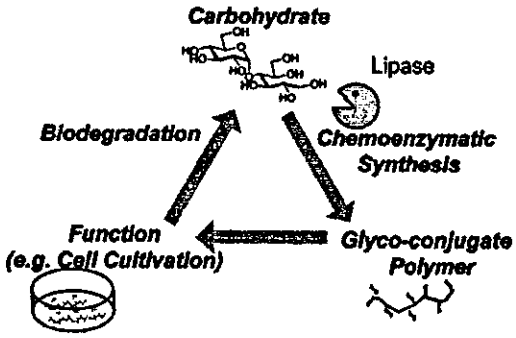

Figure 1. Schematic illustration of biomaterial via chemoenzymatic synthesis.

on the synthesis of sugar derivatives using esterases for biomaterials exhibiting biological recognition activity. In this work, we investigated a facile synthesis of a glycoconjugate polymer via enzyme-catalyzed reaction, the lectin recognition ability, the cell adhension ability, and biodegradability. Our interest in enzymatic chemoselective esterification is its application to the synthesis of biomaterials exhibiting strong binding to specific lectins, which is essential for its application as a scaffold and drug delivery system with recogntion ability to cells.

Sugar alcohols (maltitol and lactitol) were chosen as the target carbohydrate, and divinyl sebacate as an acyl donor. Since D-glucitol has been reported to show high reactivity and selectivity, the sugar alcohols are expected to show high enzymatic activity.[14] The open-chain D-glucitol moiety in maltitol might be more reactive than the α-D-Glc unit due to the less steric hindrance, and then the product modified at the D-glucitol moiety could be applicable as a starting substance to lead to a glycoconjugate polymer carrying pendant carbohydrate (Scheme 1).

Experimental Section

Materials. The following reagents were used as received. L-ascorbic acid, *N,N*-dimethylformamide (DMF), dimethyl sulfoxide (DMSO), methanol, pyridine (Kishida, Osaka),

* Corresponding author. Telephone: +81-52-789-2538. Fax: +81-52-789-2528. E-mail: miuray@mol.nagoya-u.ac.jp.

† Abbreviations: AAPD, 2,2'-azobis(2-amidinopropane) dihydrochloride; As-A, *L*-ascorbic acid; ASGPR, asialoglycoprotein receptor; ConA, concanavalin A; DMF, *N,N*-dimethylformamide; BOD, biochemical oxygen demand; DMSO, dimethyl sulfoxide; EDTA, ethylenediaminetetraacetic acid; EMEM, Eagle's minimum essential medium; FAB, fast atom bombardment; Gal, galactose; Glc, glucose; NaPyr, sodium pyruvate; NEAA, nonessential amino acids; PVA, poly(vinyl alcohol); RCA_{120}, *Ricinus communis* agglutinin 120; SEC, size exclusion chromatography; TLC, thin-layer chromatography; TOD, theoretical oxygen demand.

10.1021/bm025714b CCC: $25.00 © xxxx American Chemical Society
Published on Web 00/00/0000 PAGE EST: 5.3

Scheme 1. Synthesis of Glycoconjugate Polymers via Enzymatic Esterification of Sugar Alcohol and the Subsequent Radical Polymerization[a]

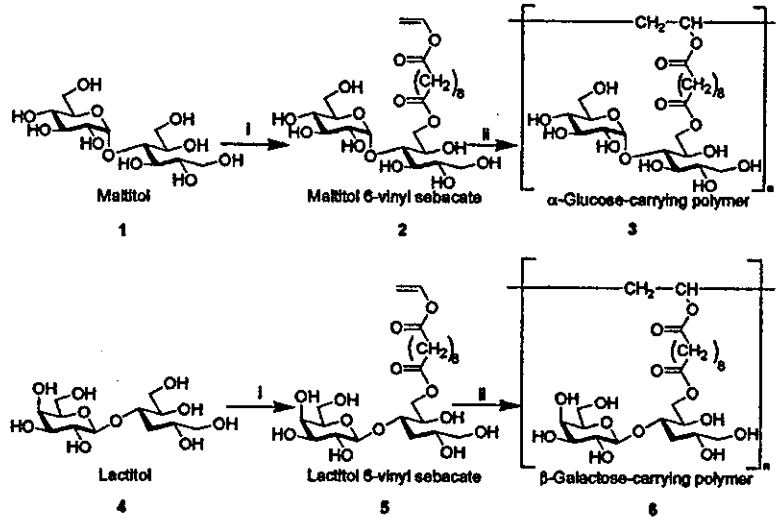

[a] Conditions: (i) divinyl sebacate, pyridine, 50 °C, 72 h, lipase; (ii) radical initiator (AAPD or H_2O_2 and *L*-ascorbic acid), H_2O/DMSO.

concanavalin A (ConA), *Ricinus communis* agglutinin 120 (RCA_{120}) (Honen Co. Ltd., Tokyo), 2,2′-azobis(2−amidinopropane)dihydrochloride (AAPD) (Wako, Osaka), 32% hydrogen peroxide (Mitsubishi Gas Chemical, Tokyo), maltitol (Tokyo Kasei, Tokyo), and lactitol monohydrate (Sigma-Aldrich, Louisiana, MO). The solvent for enzymatic esterification was dried by molecular sieve (4 Å) at least 24 h. Lipases from *Pseudomonas fluorescens* (AK), *Candida rugosa* (AY), and *Pseudomonas cepacia* (PS) were gifts from Amano Enzyme Inc. (Nagoya). The lipase from *Candida antarctica* (CA) was kindly donated by Novo Nordisk Bioindustry Ltd. The lipase from *Porcine pancreas* (PP) was purchased from Sigma-Aldrich. The lipase from *Rhizomucor miehei* (RM) was perchased from Fluka (Buchs, Switzerland).

Characterizations. ^1H (500 MHz) and ^{13}C (125 MHz) NMR spectra were recorded on a Varian Inova 500 equipped with a Sun workstation. The spectra were measured in a mixture of DMSO-d_6 and D_2O (100/1, v/v). FTIR spectra were recorded in the form of a KBr disk using a JASCO FT/IR-230. FAB mass spectra were obtained by a JEOL-JMS-AX505HA mass spectrometer using nitrobenzyl alcohol as a matrix. Fluorescence spectroscopy was carried out on a JASCO FP-777 spectrometer at 25 °C. Size exclusion chromatography (SEC) was conducted with JASCO 800 high-performance liquid chromatography on Shodex B804+B805 columns with PBS as an eluent. The molecular weights were estimated using a pullulan standard. The static contact angles of water on the prepared surfaces were measured at 25 °C operating a contact angle goniometer of Face contact-angle meter CA-D (Kyowa Interface Science Co. Ltd., Asaka, Japan).

Preparation of the Sugar Vinyl Esters. Enzyme screening was carried out with a Chemistation (EYELA, Tokyo). A mixture of 52 mg of maltitol or 54 mg of lactitol monohydrate (0.15 mmol), 0.15 g of divinyl sebacate (0.60 mmol), and 50 mg of enzyme in 1 mL of pyridine was gently stirred at 50 °C for 72 h. The conversion of sugar alcohol was estimated by high performance liquid chromatography (HPLC) on an Amide 80 column (Tosoh Co. Ltd., Kawasaki, Japan) with an eluent of acetonitrile: water: methanol (8/1/1, v/v/v), and by thin-layer chromatography (TLC). The larger-scale reaction was carried out with 0.52 g of maltitol or 0.54 g of lactitol (1.5 mmol) and 1.5 g of divinyl sebacate (6.0 mmol) in 10 mL of pyridine at 50 °C for 72 h.

Lectin Recognition Assay. Immunodiffusion was carried out with agarose, poly(ethylene glycol) and sodium azide in PBS buffer solution by the previous method.[15] The samples were allowed to diffuse for 72 h at room temperature to develop precipitation bands. Binding constants of the glycoconjugates with FITC-labeled lectins were evaluated by the Scatchard plots of the fluorescence spectroscopy.

Cell Adhesion Assay. HepG2 cell culture was carried out in EMEM supplemented with 10% fetal bovine serum, 1% NEAA, 1% NaPyr, 100 mU/mL of penicillin, and streptomycin. The surface of polystyrene dishes was treated with an aqueous solution of 1.0 mg/mL the glycoconjugate polymer prior to cell assay.[7b] The cell adhension assay was performed according to the method reported by Donati et al.[7b,16] Confluent cultures of HepG2 cells were detached using 0.025% trypsin and 0.02% EDTA and then suspended in EMEM. A hundred thousand cells were transferred into the polymer-coated polystyrene dishes and incubated at 37 °C. Nonadherent cells were removed by rinsing the dishes with PBS. Cells were then stained with 0.25% CBB (Brilliant Blue G) solution (H_2O/acetic acid/ethanol, 9/2/9, v/v/v), and rinsed with PBS. The number of cells was counted by optical microscopy.

Biochemical Oxygen Demand (BOD) Test. BOD was determined with a BOD tester (model 200F; TAITEC,

Table 1. Enzyme Screen for Esterification of Sugar Alcohols in Pyridine

enzyme	conversion (%)[a] maltitol	lactitol
lipase AK	1	93
lipase AY	0	0
lipase CA	44	99
lipase RM	21	15
lipase PS	0	13
lipase PP	5	4

[a] HPLC.

Koshigaya, Japan) by the oxygen consumption method, basically according to the JIS standard guidelines (JIS K 6950) at 25 °C using an activated sludge obtained from Nagoya municipal sewage treatment plant in Nagoya City, Japan.

Results and Discussion

Monomer Synthesis. Vinyl esters of carbohydrates can function as monomers of glycoconjugate polymers with poly(vinyl alcohol) backbone.[13] A total of six lipases (lipases AK, AY, CA, RM, PP, and PS) were screened for their capability to catalyze esterification of sugar alcohols (maltitol and lactitol) in pyridine. In both cases, no reaction occurred in the absence of enzyme. The conversion of sugar alcohol and chemoselectivity in esterification were estimated by HPLC and TLC. The results are summarized in Table 1. The conversion of sugar alcohols was modest with most of the enzymes. The lipases were more active in nonpolar solvent,[17,18] which is inapplicable to oligosaccharides due to the lack of solubility.

The conversion of lactitol was much higher than that of maltitol. The high conversion of lactitol is supposed to come from the hydration of lactitol (lactitol monohydrate is used), which might be advantageous to retain the activity of the enzymes.[18] In addition, the hydrophobicity of α-anomeric surface in the galactose moiety might be more preferable than glucose as a substrate. The best lipase was lipase CA.

In lactitol and maltitol, there are eight hydroxyl groups, thereby requiring chemoselective esterification prior to use as monomers. To that end, larger-scale reactions were performed with lipase CA. The resultant compound was purified by the column chromatography, and the chemoselectivity was confirmed by ^{13}C NMR, in which the chemical shifts of esterified carbons have been reported to show a downfield shift.[9,19] In the ^{13}C NMR of maltitol, three peaks were observed at δ 61.6, 63.5, and 63.9 ppm due to the primary hydroxymethylenes at the 6', 1, and 6 positions, respectively. In the ^{13}C NMR of the resultant product with lipase CA, the methylene group at the C6 position alone was shifted to a lower magnetic field (δ 66.7 ppm), indicating that the chemoselective esterification proceeded (Figure 2). The disubstituted compound was not obtained with lipases.[20] The chemoselectivity of lactitol was also confirmed by the same method.[21]

The enzymatic esterification of polyol was reported to be affected by the steric hindrance around the hydroxyl group, and the substitutions of the primary and secondary alcohols

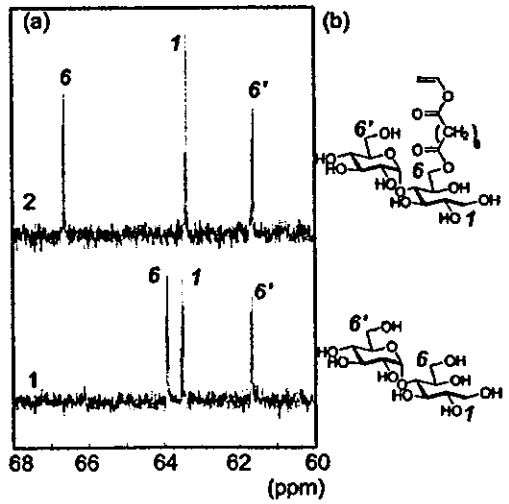

Figure 2. (a) Expanded ^{13}C NMR of the esterified maltitol by lipase CA (top) and maltitol (bottom) and (b) corresponding chemical structures.

are remarkably discriminated.[22] Glucitol has an open-chain structure and the hydroxyl groups at C1 and C6 are highly reactive with lipases. In the case of maltitol and lactitol, lipase CA showed an outstanding selectivity to the hydroxyl group at the C6 position, but not to that at the C1 position.

Polymerization of Sugar Alcohol Esters. The resultant vinyl esters of the sugar alcohols (**2** and **5**) were polymerized by a free radical initiator using 2,2'-azobis(2−amidinopropane) dihydrochloride (AAPD) or hydrogen peroxide with L-ascorbic acid (As-A).[23] The results of the polymerization are summarized in Table 2. The monomers have an amphiphilic structure with longer alkyl chains, and the solubility was poor in many solvents, which made polymerization difficult. **2** was soluble only in water and DMSO, and **5** was soluble a little only in DMSO. Suspension polymerization of **2** proceeded in water with AAPD and hydrogen peroxide/As-A. Suspension polymerization of **5** proceeded in a mixture of water and DMSO only with hydrogen peroxide/As-A. Despite insolubility of monomers, the resulting polymers, **3** and **6**, were readily soluble in water, suggesting the glycocluster formation due to the amphiphilic structure composed of sebacate and carbohydrate.[8] Their molecular weights were on the order of 10^4. The polymers obtained with hydrogen peroxide/As-A (run nos. 4 and 10 in Table 2) were used in the biological assay.

Lectin Recognition Ability. To evaluate the biological ability of the polymers (**3** and **6**), we investigated the affinities with lectins by means of the two-dimensional immunodiffusion test in agar and fluorescence spectrometry (Table 3).

Two-dimensional immunodiffusion tests were carried out using ConA (α-Glc binding lectin) and RCA_{120} (β-Gal binding lectin). Sharp precipitation bands appeared on the gel between ConA and **3** and between RCA_{120} and **6**. Other combinations did not show any precipitation bands, which indicates the specific interactions of glycopolymers with lectins. In addition, sugar alcohols and monomers did not show any bands, indicative of the glyco-cluster effects.

Table 2. Polymerization of Maltitol 6-Vinyl Sebacate (2) and Lactitol 6-Vinyl Sebacate (5)[a]

run no.	monomer	solvent (mL) H_2O/DMSO	AAPD[b] (mol %)	H_2O_2 (%)	As-A[c] (mM)	yield (%)	M_n ($\times 10^{-4}$)	M_w/M_n
1[d]	2	0.11/0.0	1.0			>99	1.5	3.2
2[d]	2	0.12/0.10	1.0			54	0.69	1.6
3[e]	2	0.0/0.20	1.0			0		
4[e]	2	0.20/0		0.032	10	35	2.8	2.6
5[d]	2	0.0/0.20		0.032	10	0		0
6[d]	5[f]	0.20/0.0	1.0			0		
7[b]	5[f]	0.10/0.10	1.0			0		
8[b]	5[f]	0.0/0.20	1.0			0		
9[e]	5[f]	0.20/0.0		0.032	10	49	2.0	1.9
10[e]	5[f]	0.10/0.10		0.032	10	82	1.3	1.7
11[e]	5[f]	0.0/0.20		0.032	10	0		

[a] 10 mg of monomer. [b] 2,2'-Azobis(2-amidinopropane) dihydrochloride. [c] L-Ascorbic acid. [d] Temperature: 60 °C. Time: 20 h. [e] Temperature: 35 °C. Time: 2.5 h. [f] Suspension polymerization.

Table 3. Estimation of Lectin Recognition Abilities

	immunodiffusion[a]		affinity constant (M^{-1})[b,c]	
	conA	RCA_{120}	conA	RCA_{120}
1	−	−	2.1×10^3	n.d.
3[d]	+	−	7.0×10^4	n.d.
4	−	−	n.d.	1.4×10^3
6[e]	−	+	n.d.	6.1×10^4
PVLA[f]	−	+	n.d.	1.3×10^5

[a] The appearance of a precipitation band is shown by (+), and no precipitation band, by (−). [b] The affinity constants are based on the molarity of the glycosyl unit. [c] "n.d."means "not detectable". [d] α-Glc polymer run no. 4 in Table 2. [e] β-Gal polymer run no. 10 in Table 2. [f] $M_n = 5.9 \times 10^4$; $M_w/M_n = 1.7$.

Lectins were precipitated through specific cross-linking with carbohydrate ligands along the polymer chain. The results showed the specific and strong interaction of the polymers (**3** and **6**) with the corresponding lectins.

The binding affinities of the polymers for the lectins were investigated by fluorescent spectroscopy using FITC-labeled lectins (Figure 3). The fluorescence was decreased with the addition of these polymers. The relative change in the fluorescent intensity ($\Delta F/F_o$) at 518 nm was plotted against the carbohydrate concentration. The association constants were estimated by the Scatchard plot as follows:

$$\frac{[\alpha\text{-Glc or }\beta\text{-Gal}]F_o}{\Delta F} = \frac{[\alpha\text{-Glc or }\beta\text{-Gal}]F_o}{\Delta F_{max}} + \frac{F_o}{\Delta F_{max}K_a}$$

where [α-Glc], [β-Gal], K_a, F_o, ΔF, and ΔF_{max} represent the concentration of the α-Glc solution (M), the concentration of the β-Gal solution (M), the association constant (M^{-1}), the initial fluorescent intensity, the fluorescent change, and the maximum fluorescent change, respectively.

3 and **6** showed specific affinities to ConA and RCA_{120}, respectively, and the affinity constants were much higher than those for the sugar alcohols, indicating again the glycocluster effect. Interestingly, the affinities of sugar alcohols were very weak though they have molecular regognition unit. Though the affinities of **6** to RCA_{120} was lower than that of polystyrene type of glycoconjugate polymer (PVLA: as control) (Figure 4),[7] the neoglyoconjugates with PVA backbone (**6**) showed strong interactions with lectins, and have a potential to application for biomaterials.

Cell Adhesion Assay. Prior to the cell adhesion assay, polystyrene dishes were treated with aqueous solutions of

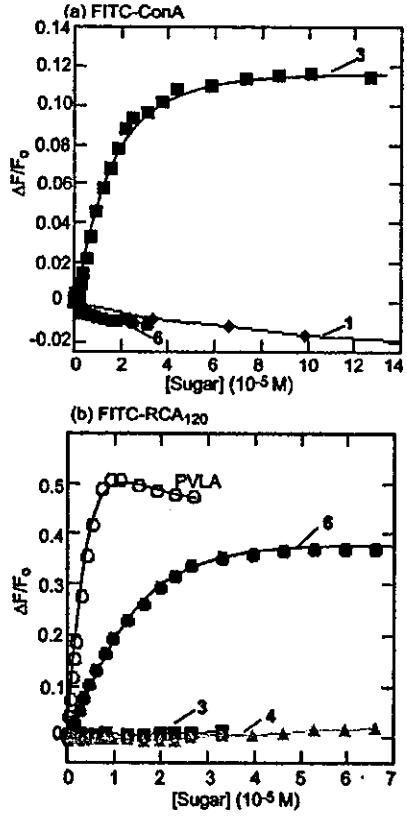

Figure 3. Fluorescence intensity changes of FITC-labeled lectins with varying sugar concentration. (a) ConA and (b) RCA_{120}.

glycoconjugate polymers. Because of the amphiphilic structure, the glycopolymers could be adsorbed to polystyrene dishes by hydrophobic interaction. The adsorption of glycopolymers onto polystyrene was confirmed by the decrease of the contact angles of the surface (Table 4).

As shown in Figure 5, a **6**-coated polystyrene dish stimulated the adhension of HepG2 more effectively than **3**-coated and noncoated polystyrene dishes. These results suggest that the asialoglycoprotein receptor (ASGPR) plays a key role as a scaffold of hepatocytes on **6**-coated dishes, in contrast to nonspecific interaction of hepatocytes on the other dishes.[7b,16]

Micropatterned Carbohydrate Displays by Self-Assembly of Glycoconjugate Polymers on Hydrophobic Templates on Silicon

Yoshiko Miura,*,† Hajime Sato,† Takayasu Ikeda,† Hiroyuki Sugimura,‡ Osamu Takai,‡ and Kazukiyo Kobayashi†

Department of Molecular Design and Engineering and Department of Materials Processing Engineering, Graduate School of Engineering, Nagoya University, Furo-cho, Chikusa-ku, Nagoya 464-8603, Japan

Received February 16, 2004; Revised Manuscript Received June 5, 2004

We report a novel strategy for micropatterned carbohydrate displays on Si substrates. This method exploited the hydrophobic−hydrophilic microfabrication by photolithography of ODS-SAM on Si substrates and the subsequent selective self-assembly of glycoconjugate polymers onto the hydrophobic regions. Protein micropatterning by molecular recognition on the carbohydrate substrates was also successful.

Introduction

Micropatterned biomacromolecules on solid surfaces have been fabricated for a variety of applications to support the progress of biotechnology. For instance, micropatterned DNAs are extensively used to analyze a vast amount of genes simultaneously.[1,2] Micropatterned proteins are exploited for cell cultivation and biosensors.[3,4] Micropatterned carbohydrates on solid surfaces are expected to analyze carbohydrate−protein interactions and to fabricate the scaffolds of cell cultivation,[5−8] because carbohydrates on cell surfaces play important roles in numerous intercellular recognition processes.[9] Since carbohydrate−protein interactions are usually weak and amplified with multivalent effects,[10] it is important to exploit a strategy for micropatterning of carbohydrate on solid surfaces with the multivalency.

Both "bottom-up" (self-assembly of molecules) and "top-down" (lithography of substrates) processes have been developed to fabricate micropatterned biomolecules on solid surfaces. Self-assembled monolayers (SAMs) on surfaces are paid attention for fabrication of nanomaterials due to their well-defined structures[11] and applicabilities.[12,13] Photolithography of substrate is most practical among various patterning methods and has been applied to the development of microdevices such as electronic circuits and microelectromechanical systems (MEMS), since it can transfer an entire pattern to substrates through a photomask.[14] Combinations of the self-assembly of molecules and lithography of substrates are promising methods for fabricating microstructures on solid surfaces.[15,16]

In this paper, micropatterned displays of carbohydrates on silicon surfaces have been accomplished by a combination of "bottom-up" and "top-down" approaches according to the process illustrated in Figure 1. Here, the well-ordered SAM of octadecyltrimethoxysilane (ODS) on silicon substrates was micropatterned by photolithography using vacuum ultraviolet (VUV) light. Since VUV light of 172 nm wavelength excites and decomposes C−C and C−H bonds, all organic molecules are able to be micropatterned by the photolithography of VUV light.[14] The well-defined hydrophobic−hydrophilic

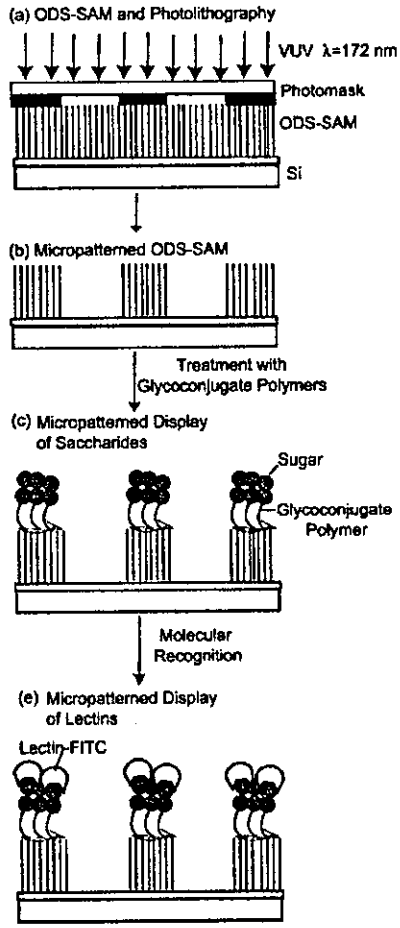

Figure 1. Schematic illustration of micropatterned display: (a) photolithography on ODS-SAM, (b) micropatterned ODS-SAM, (c) micropatterned display of carbohydrate, and (d) micropatterned display of lectin.

* To whom correspondence should be addressed. Telephone: +81-52-789-2538. Fax: +81-52-789-2528. E-mail: miuray@mol.nagoya-u.ac.jp.
† Department of Molecular Design and Engineering.
‡ Department of Materials Processing Engineering.

10.1021/bm049904t CCC: $25.00 © xxxx American Chemical Society
Published on Web 00/00/0000 PAGE EST: 5.7

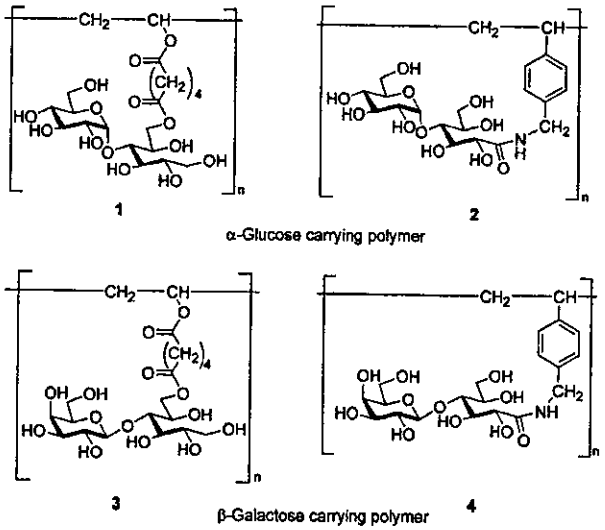

Figure 2. Molecular structures of the glycoconjugate polymers.

micropattern was modified by self-assembly of amphiphilic glycoconjugate polymers, and the micropatterned carbohydrate display was visualized by molecular recognition of lectins with fluorescein isothiocyanate (FITC) fluorophore.[17]

Glycoconjugate polymers, each carrying α-Glc (**1** and **2**) and β-Gal (**3** and **4**) as recognition signals, were employed in this paper (Figure 2).[18] Hydrophilic carbohydrate residues are attached to every repeating unit along the hydrophobic polymer backbones (poly(vinyl alcohol) and polystyrene). Owing to the amphiphilic characters, these polymers take characteristic conformations in water and also they are strongly adsorbed to hydrophobic solid surfaces.[19] It is also important that the highly concentrated or clustered carbohydrate residues serve as strong recognition signals to express a variety of biological functions. In addition to these characteristics, the glycopolyvinyl sebacates (**1** and **3**) were biodegradable.

Experimental Section

Materials. Glycoconjugate polymers were synthesized following our previous methods (**1**: $M_n = 0.80 \times 10^4$, $M_w/M_n = 1.7$; **2**: $M_n = 1.0 \times 10^4$, $M_w/M_n = 1.4$; **3**: $M_n = 1.5 \times 10^4$, $M_w/M_n = 1.8$; **4**, $M_n = 1.7 \times 10^4$, $M_w/M_n = 2.4$).[18,20] Concanavalin A (Con A; α-Glc binding lectin), *Ricinus communis* agglutinin 120 (RCA_{120}; β-Gal binding lectin) (Honen Co. Ltd., Tokyo), and bovine serum albumin (BSA) (Amersham Bioscience, Uppsala, Sweden) were used as received.

Measurements. The static contact angle of water on the prepared surfaces was measured at 25 °C by operating a drop shape analysis system of DSA 10 Mr2 (Krüss, Germany). The thickness of the film on Si(100) substrate was measured with a PZ2000 ellipsometer (Philips, Holland) using a He–Ne laser of 632.8 nm, in which the incident angle was 70° from the normal. The FTIR spectra in the transmission method under a N_2 atmosphere were recorded with an FTIR 7000 (Digilab Laboratories, USA) with 1000 times of interferogram accumulation. The surface plasmon resonance (SPR) measurements were performed with a SPR 670 (Nippon Laser & Electronics Labs, Japan). Fluorescence spectroscopy was carried out on a JASCO FP-777 spectrometer at 25 °C. XPS analysis was performed using an ESCA-3300 (Shimadzu/Kratos, Kyoto, Japan) with a collection angle of 45° from the normal. Scanning electron microscopy (SEM) was performed with a JSM-6330F (JEOL Ltd., Japan). Fluorescence microscopic studies were performed using a Zeiss Axiover 200 M laser confocal microscope (Carl Zeiss Inc., Germany) equipped with external argon laser (for excitation at 490 nm).

Preparation and Photolithgraphy of ODS-SAM.[14,15] Well-defined ODS-SAM was prepared by the chemical vapor deposition (CVD) method. A silicon substrate was cleaned by UV/ozone irradiation. The cleaned silicon substrate and a glass cup containing ODS liquid were placed in a Teflon container. The container was sealed with a cap and heated in an oven at 150 °C for 4 h. ODS was vaporized and allowed to react with silanol groups on the substrate surface to give ODS-SAM. Formation of ODS-SAM was confirmed by the increase of contact angle from 0° to 103.8°, and the thickness estimated by ellipsometry was 15 Å.

Micropatterned SAM samples were prepared by photolithography. A selected region of ODS-SAM was photochemically decomposed and removed by irradiation with VUV light (excimer lamp, Ushio Inc., UER20-172V, λ = 172 nm and 10 mW/cm^2) through a photomask under a reduced pressure of 10 Pa for 30 min.

Glycoengineering and Lectin Binding on the Micropatterned Surface. The patterned ODS-SAM substrates were incubated in an aqueous solution of the glycoconjugate polymers (**1**–**4**) (0.5 mg/mL) at room temperature for 5 h. The substrate was rinsed thoroughly with distilled water and dried in a stream of nitrogen gas and under vacuum. The resultant polymer-coated substrate was incubated with FITC-labeled lectin (Con A and RCA_{120}) in 1 mg/mL phosphate-buffered saline (PBS) solution at room temperature for 2 h, and then washed with PBS to remove weakly bound substance. The fluorescence image was recorded with a fluorescence microscope and analyzed with Scion image software (version 4.02 beta, Scion Co., Frederick, MD).

Lectin Recognition Assay. The binding constants of the glycoconjugate polymers with lectins were evaluated on substrates by surface plasmon resonance and in aqueous solutions by fluorescence spectroscopy.

To evaluate the lectin recognition ability on substrates, surface plasmon resonance (SPR) measurements were performed at 25 °C with a flow rate of 15 μL/min, in which SAM of ocatadecylmercaptan on gold was used instead of ODS-SAM, and the glycoconjugate polymers were adsorbed on the SAM to evaluate the binding constants on the substrates. Kinetic and binding constants were calculated from the sensorgrams with SPR software (SPR Processing, version 4.00, Nippon Laser & Electronics Labs). Langmuir binding between the glycopolymer and lectin (glycopolymer + lectin → glycopolymer–lectin) was assumed in the calculation. The glycopolymer-coated substrate was used as the control in SPR analysis.

In an aqueous solution, the relative change of the fluorescent intensity ($\Delta F/F_0$) at 518 nm was plotted against

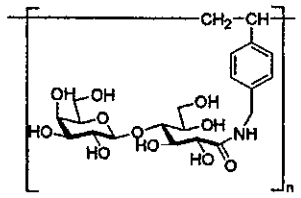

PVLA

Figure 4. Lactose-carrying polystyrene (**PVLA**).

Table 4. Contact Angles of the Polymer Coated Dishes[a]

polymer	contact angle (deg)
3	60
6	61
polystyrene (control)	75

[a] The polystyrene dishes were treated with the glycoconjugate polymer solution of 1.0 mg/mL for 13 h.

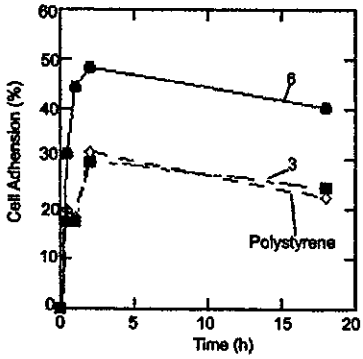

Figure 5. Cell adhension efficiency on the polymer coated dishes.

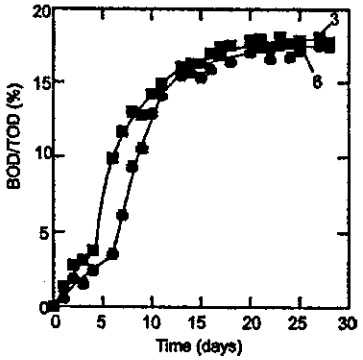

Figure 6. Biodegradability of the glyco-conjugate polymers (**3** and **6**) with PVA backbone.

Biodegradability. These glycoconjugate polymers consist of biodegradable dicarboxylic ester of PVA, and carbohydrates. The biodegradability of the polymers was evaluated by the biochemical oxygen demand (BOD)/theoretical oxygen demand (TOD) value using the oxygen consumption method (Figure 6).

The biodegradabilities of **3** and **6** were modest, but much improved from PVA (less than 5%).[13,24] Figure 7 is the FTIR spectra of **3** and **6** before and after the degradation. The strong adsorption of alkyl chain and ester bond around 2950

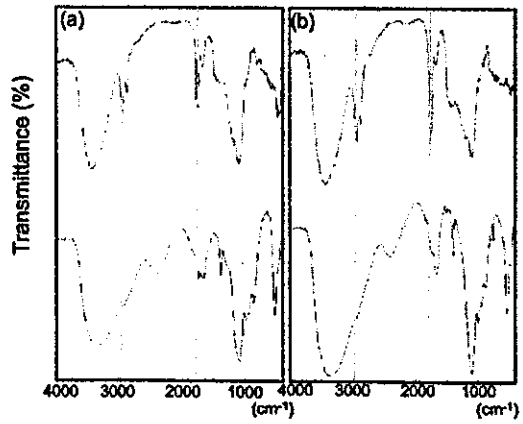

Figure 7. FTIR spectra of (a) **3** and (b) **6** before (top) and after (bottom) biodegradation.

and 1730 cm^{-1} decreased after biodegradation, which suggests that pendant carboxylic acid and sugar alcohol moieties are degraded with preference. The biodegradability of **3** and **6** implies that these glycoconjugate polymers are useful not only as biomaterials but also as green materials which can be regarded as a chemical recycling system for biomaterials.

Conclusion

Novel glycoconjugate polymers were synthesized via a facile chemoenzymatic reaction. The lipase catalyzed esterification of sugar alcohols (maltitol and lactitol) with divinyl sebacate provided sugar vinyl ester. With lipase from *C. antarctica*, maltitol 6-vinyl ester and lactitol 6-vinyl ester were obtained at high yield and chemoselectivity. The sugar vinyl esters were successfully polymerized into glycoconjugate polymers of poly(vinyl alcohol) derivatives with hydrogen peroxide and L-ascorbic acid initiator. The glycoconjugate polymers showed strong and specific interactions with lectins and hepatocytes due to the multivalency. The biodegradability of the gycoconjugate polymers were modest but higher than PVA. It is important to note that the chemoenzymatic synthesis can be a new method for biomaterial fabrication.

Acknowledgment. This work was supported by a Grant-in-Aid for Young Scientist (B) and by the Japan Chemical Innovation Institute (JCII), Hattori-Hokokai Foundation, Sekisui Integrated Research Foundation, and Eno Science Foundation. The authors are grateful to Prof. Shiro Kobayashi, and Prof. Hiroshi Uyama (Kyoto University) for helpful discussion on enzymatic synthesis, to Dr. Yoshihiro Ito (Kanagawa Academy of Science and Technology) for helpful support on the biological assay, and to Prof. Keigo Aoi (Nagoya University) for helpful support on the BOD experiment.

Supporting Information Available. Text giving characterization information and spectral data for **2** and **5**, and a figure showing the expanded ^{13}C NMR spectra of **4** and **5** for estimation of chemoselectivity. This material is available free of charge via the Internet at http://pubs.acs.org.

References and Notes

(1) Varki, A. *Glycobiology* **1993**, *3*, 97.
(2) For example: Lee, R. T.; Ichikawa, Y.; Fay, M.; Drickamer, K.; Shao, M. C.; Lee, Y. C. *J. Biol. Chem.* **1991**, *266*, 4810.
(3) Lee, Y. C. *Carbohydr. Res.* **1978**, *67*, 509.
(4) (a) Lee, R. T.; Lee, Y. C. *Neoglycoconjugates: Preparations and Applications*: Lee, Y. C., Lee, R. T., Eds.; Academic: San Diego, CA, 1994; pp 23−50. (b) Lee, Y. C.; Lee, R. T. *Acc. Chem. Res.* **1995**, *28*, 321.
(5) Lainé, V.; Coste-Sarguet, A.; Gadelle, A.; Defaye, J.; Perly, B.; Djudami-Pilard, F. *J. Chem. Soc., Perkin Trans. 2* **1995**, *11*, 1479.
(6) Roy, R.; Kim, J. M. *Angew. Chem., Int. Ed. Engl.* **1999**, *38*, 369.
(7) (a) Kobayashi, K.; Sumitomo, H.; Ina, Y. *Polym. J.* **1985**, *17*, 567. (b) Kobayasi, A.; Akaike, T.; Kobayashi, K.; Sumitomo, H. *Makromol. Chem., Rapid Commun.* **1986**, *7*, 645. (c) Tsuchida, A.; Kobayashi, K.; Matsubara, N.; Muramatsu, T.; Suzuki, T.; Suzuki, Y. *Glycoconjugate J.* **1998**, *15*, 1047.
(8) Wataoka, I.; Urakawa, H.; Kajiwara, K.; Kobayashi, K. *Macromolecules* **1999**, *32*, 1816.
(9) (a) Therisod, M.; Klibanov, A. M. *J. Am. Chem. Soc.* **1986**, *108*, 5638. (b) Therisod, M.; Klivanov, A. M. *J. Am. Chem. Soc.* **1987**, *109*, 3977. (c) Sergio, R.; Chopineau, J.; Kieboom, A. P. G.; Klibanov, A. M. *J. Am. Chem. Soc.* **1988**, *110*, 584.
(10) Gross, R. A.; Kumar, A.; Karla, B. *Chem. Rev.* **2001**, *101*, 2097.
(11) Kobayashi, S.; Uyama, H.; Kimura, S. *Chem. Rev.* **2001**, *101*, 3793.
(12) Chen, X.; Martin, B. D.; Neubauer, T. K.; Linhardt, R. J.; Dordick, J. S.; Rethwisch, D. G. *Carbohydr. Polym.* **1995**, *28*, 15.
(13) (a) Tokiwa, Y.; Fan, H.; Hiraguri, Y.; Kurane, R.; Kitagawa, M.; Shibatani, S.; Maekawa, Y. *Macromolecules* **2000**, *33*, 1636. (b) Kitagawa, M.; Tokiwa, Y. *Biotechnol. Lett.* **1998**, *20*, 627.
(14) Uyama, H.; Klegraf, E.; Wada, S.; Kobayashi, S. *Chem. Lett.* **2000**, 800.
(15) Kobayashi, K.; Akaike, T. *Trends Glycosci. Glycotechnol.* **1990**, *2*, 26.
(16) Donati, I.; Gamini, A.; Vetere, A.; Campa, C.; Paoletti, S. *Biomacromolecules* **2002**, *3*, 805.
(17) Klivanov, A. M. *CHEMTECH* **1986**, *16*, 354.
(18) Gorman, L. A. S.; Dordick, J. S. *Biotechnol. Bioeng.* **1992**, *39*, 392.
(19) Yoshimoto, K.; Itatani, Y.; Tsuda, Y. *Chem. Pharm. Bull.* **1980**, *28*, 2065.
(20) Maltitol 6,6′-divinyl sebacate (2%) and lactitol 6,6′-divinyl sebacate (3%) was obtained in the case of protease from *Bacillus sp.*
(21) The analytical data of the compounds are available in the Supporting Information.
(22) Halldorsson, A.; Magnusson, C. D.; Haraldsson, G. G. *Tetrahedron Lett.* **2001**, *42*, 7675.
(23) Larpent, C.; Tadros, T. F. *Colloid Polym. Sci.* **1991**, *269*, 1171.
(24) Takasu, A.; Itou, H.; Takada, Y.; Inai, Y.; Hirabayashi, T. *Polymer* **2002**, *43*, 227.

BM025714B

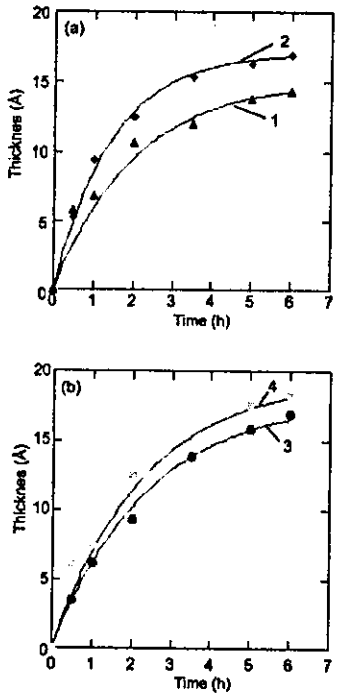

Figure 3. Thicknesses of the glycoconjguate polymers (**1**–**4**) of ODS-SAM on Si substrate estimated by ellipsometry: (—) calulation according to Langmuir Isotherms.

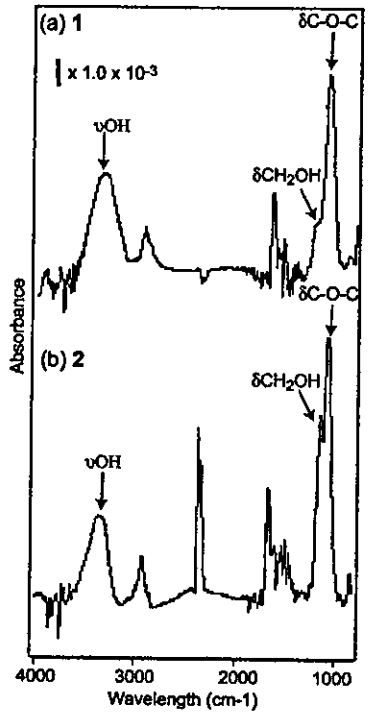

Figure 4. FTIR spectra on Si substrate: (a) **1**-coated ODS-SAM and (b) **2**-coated ODS-SAM.

the carbohydrate concentration. The association constants were estimated by the Scatchard plot as follows:[20]

$$\frac{[\text{sugar}]F_o}{\Delta F} = \frac{[\text{sugar}]F_o}{\Delta F_{max}} + \frac{F_o}{\Delta F_{max}K_a}$$

where [sugar], K_a, F_o, ΔF, and ΔF_{max} represent the concentration of the sugar unit (α-Glc or β-Gal) (M) of the polymer, the association constant (M^{-1}), the initial fluorescent intensity, the fluorescent change, and the maximum fluorescent change, respectively.

Result and Discussion

Adsorption of the Glycoconjugate Polymers on ODS-SAM.[21] The adsorption behaviors of the glycoconjugate polymers were studied with ODS-SAM before applying photolithography. Immersing an ODS-SAM substrate in an aqueous solution of glycoconjugate polymer decreased the contact angles on the substrate: unreacted ODS-SAM, 103.8°; treated with **1**, 70.5°; treated with **2**, 78.2°; treated with **3**, 73.8°; treated with **4**, 79.3°. The thicknesses of the polymer layers estimated by ellipsometry were increased with the immersion to reach 15–20 Å after 5–6 h irrespective of the polymer backbones and sugar structures, and the time courses of the polymer adsorption were followed by the Langmuir equation (Figure 3).[22] Typical bands due to carbohydrates of the polymer-coated ODS-SAM on Si were observed by FTIR in Figure 4: ν(O–H, broad peak around 3400 cm^{-1}), δ(C_6–O–H around 1250 cm^{-1}), and δ(C–O–C, carbohydrate ring, around 1100 cm^{-1}).[23] XPS observation of the polymer-coated ODS-SAM is described in a later section. On the other hand, the glycoconjugate polymers were little adsorbed on bare hydrophilic Si. It is suggested that these glycoconjugate polymers were specifically adsorbed on the hydrophobic ODS-SAM by the interaction between the polymer backbone and substrate and that the saccharide moieties of the polymers were exposed to the surface.

Lectin Recognition on Substrates. The affinities of Con A and RCA_{120} lectins to the glycopolymer-coated substrates were estimated by SPR (Figure 5). Strong and specific responses of Con A to **1** and **2** and RCA_{120} to **3** and **4** were observed in the SPR shift angles. Typically, the maximum SPR shift angle of Con A to **2** was 7 times that of RCA_{120} to **2** and 50 times that of BSA to **2**. The sensorgrams of **2** and **4** with polystyrene backbone showed a more rapid rise in the association phase and a more rapid downturn in the dissociation phase than those of **1** and **3** with poly(vinyl alcohol) backbone. The association of RCA_{120} to **4** was much faster than that of Con A to **2**. These observations can be evaluated by the kinetic treatments of the sensorgrams, which gave the association and dissociation rate constants (k_a and k_d) and association constant (K_a) as summarized in Table 1.

Nonspecific interactions K_a (M^{-1}) of BSA to the glycopolymer-coated substrates evaluated with the SPR software were weak: **1**, 2.5×10^{-1}; **2**, 4.1×10^{-1}; **3**, 1.0×10^{-2}; **4**, 5.3. On the other hand, nonspecific interactions of the lectins to the octadecylmercapto-SAM were much strong without specificity (Con A, 6.6×10^6; RCA_{120}, 1.1×10^7; BSA, 8.6×10^5 (M^{-1})).[24,25]

The specific and strong interactions of the lectins to the polymer-coated substrates can be discussed with respect to the association constants. The glycopolymers with polystyrene backbone were superior in both interaction and specificity to those with poly(vinyl alcohol) backbone. The protein–carbohydrate interactions are affected not only by the

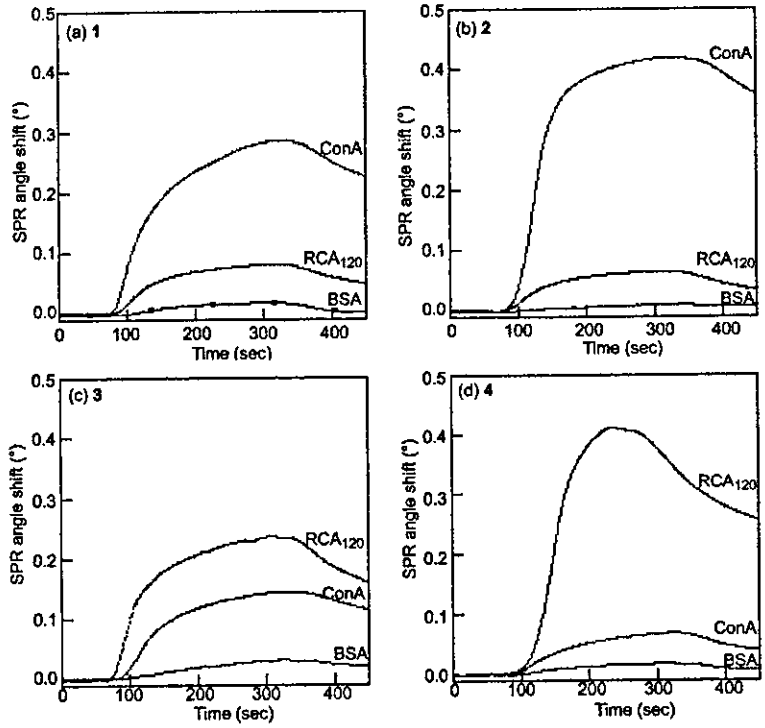

Figure 5. SPR analyses of Con A, RCA_{120}, and BSA affinities to polymer-coated substrates (1–4) at 25 °C.

Table 1. Association and Dissociation Rate Constants and Equilibrium Association Constants of the Polymer-Coated Surfaces to Lectins by SPR

	Con A			RCA_{120}		
	k_a (M^{-1} s^{-1})	k_d (s^{-1})	K_a (M^{-1})	k_a (M^{-1} s^{-1})	k_d (s^{-1})	K_a (M^{-1})[a]
1	1.9×10^3	3.7×10^{-3}	5.2×10^5	10.0	6.2×10^{-3}	1.6×10^3
2	4.7×10^5	1.3×10^{-3}	3.6×10^8	2.3	1.1×10^{-2}	2.2×10^2
3	8.4	1.1×10^{-2}	7.6×10^2	1.3×10^3	8.0×10^{-3}	1.6×10^5
4	5.9	1.2×10^{-2}	4.9×10^2	1.7×10^6	3.3×10^{-2}	5.2×10^7

Table 2. Association Constants of Glycoconjugate Polymers with Lectins in Aqueous Solution by Fluorescence Spectroscopy

	K_a[a] (M^{-1})	
	Con A	RCA_{120}
maltitol	1.1×10^3	n.d.[b]
1	3.6×10^5	9.5×10^3
2	4.5×10^5	1.4×10^3
3	7.4×10^3	2.6×10^4
4	2.4×10^3	1.3×10^5

[a] The affinity constants are based on the molarity of glycosyl unit. [b] n.d., not detectable.

saccharide structures but also by the glyco cluster scaffold. The influence of the glyco scaffold on the lectin recognition has been pointed out by our group[18,26] and other groups.[27,28]

Lectin affinities of the polymers in aqueous solutions were estimated by fluorescence spectroscopy for comparison (Table 2). Specific and strong interactions in aqueous solutions (Con A to **1** and **2**, and RCA_{120} to **3** and **4**) were observed as well as those on the substrate. The affinities were much stronger than those of isolated sugar due to the glyco cluster effects of the polymers. The glycopolymers on the substrate showed stronger interactions with lectins than those in aqueous solution, which indicated the polymer-coated substrates maintain and amplify the glyco cluster effects of the polymers.

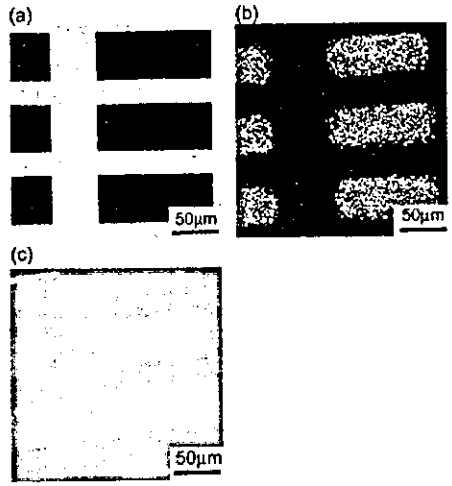

Figure 6. Optical micrographs on Si substrate: (a) photomask used and (b) the micropatterned ODS-SAM stained with water vapor. (c) SEM of **1**-coated substrate.

Micropatterned Adsorption of Glycoconjugate Polymers. Hydrophobic–hydrophilic micropatterned ODS-SAM was prepared by photolithography using VUV light at 172 nm. The decomposition of ODS by photoirradiation was confirmed by the decrease of contact angle of the substrate and also visualized by optical micrographs (Figure 6a,b).

Then the micropatterned ODS-SAMs were immersed in aqueous solutions of glycoconjugate polymers. SEM suggests that the glycoconjugate polymer was adsorbed on ODS-SAM region (Figure 6c). The representative XPS spectra of the polymer-coated substrates on the ODS-SAM are shown in Figure 7.[29] The C 1s spectra were resolved by the pseudo-

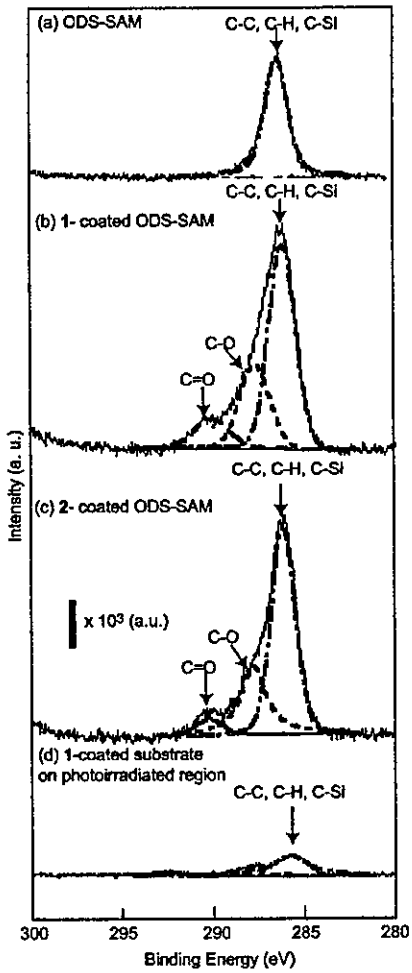

Figure 7. XPS spectra on Si substrate: (a) ODS-SAM, (b) **1**-coated ODS-SAM, (c) **2**-coated ODS-SAM, and (d) **1**-coated substrate on photoirradiated region.

Voigt function. In the ODS-SAM (Figure 7a), the main peak around 286.3 eV was assigned to C−C, C−H, and C−Si bands. The polymer-coated ODS-SAM (Figure 7b,c) showed shoulders around 288.5 and 290.5 (eV) in the C 1s region, which corresponded to the C−O of saccharides and esters and C=O of esters and amide of the polymer side chains. On the other hand, the intensities of C−O and C=O peaks on the photodegraded region were almost 10% of those on ODS-SAM (Figure 7d), indicating the selective adsorption of the polymers on the micropatterned substrate.

Micropatterned Lectin Displays on the Glycoconjugate Polymer Substrates. The lectin recognition of the micropatterned carbohydrates was visualized by fluorescence microscopy using FITC-labeled lectin (Figure 8). Fluorescence images were observed along the micropatterns, and the patterning was specific to the combination between carbohydrates and lectins (**1** and **2** to Con A, and **3** and **4** to RCA_{120}).

The lectin patterning to glycopolymer-coated substrates on ODS-SAM was assessed by XPS and fluorescent intensity.[30] The atomic percentages of N 1s/C 1s were in the range of 0.22−0.30 for the specific combinations of Con A to **1** and **2** on ODS-SAM and of RCA_{120} to **3** and **4** on ODS-SAM. These values were not high enough to be compared

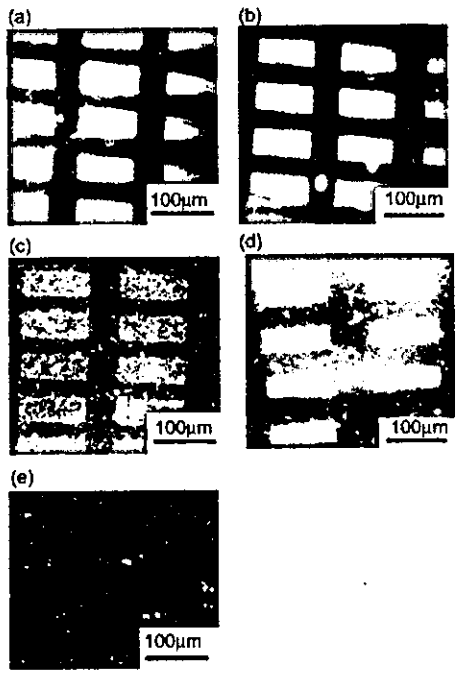

Figure 8. Fluorescence micrographs on Si substrate: (a) Con A on **1**-coated ODS-SAM, (b) Con A on **2**-coated ODS-SAM, (c) RCA_{120} on **3**-coated ODS-SAM, (d) RCA_{120} on **4**-coated ODS-SAM (negative pattern), and (e) RCA_{120} on **1**-coated ODS-SAM (discordant combination).

with 0.16 for Con A to **1** on photodegraded ODS. The fluorescent intensity ratios of the micropatterned region to the background photodegraded region were in the range of 1.8−2.3 for the specific combinations. The contrast of patterning of the lectins was not complete, compared to the high contrast or selective adsorption of the glycoconjugate polymers to ODS-SAM as suggested by XPS peak intensity ratio (Figure 7). The shapes of the fluorescence images were also slightly different from each other (Figure 8a−d) due to the nonspecific adsorption of protein. The blocking method is required to attain the better lectin patterning.

Photolithography,[31] microcontact printing,[32] and spotting[33] are well established and utilized for a variety of biomacromolecular micropatternings. However, these micropatternings are affected by substrate properties, photochemical processes, and ambient conditions. The self-assembly of biomacromolecules is another potential approach of patterning to modify the surface properties,[34] and the self-assembly in aqueous solution by hydrophobic interaction and molecular recognition is a universal driving force for formation of microstructures, which applies to a variety of molecules and substrates.

Conclusions

We have proposed a new method for micropatterned carbohydrate displays, which are achieved by the self-assembling of the glycoconjugate polymers on the hydrophobic micropatterns prepared via photolithography of ODS-SAM. Lectins were also selectively adsorbed on the carbohydrate displays to form micropatterned proteins.

This patterning strategy is based on the self-assembly of biomacromolecules, and is applicable for a variety of

substrates such as ceramics, metals, and polymers. The micropatterning via hydrophobic−hydrophilic templates is useful for the fabrication of micropatterned biomacromolecules and nanomaterials. The combination of the top-down material processing (lithography) and the bottom-up processing (self-assembly of the biomacromolecules) is one of the key methodologies for the nanomaterials. Carbohydrate microchips and patterned cell cultivations using this strategy are currently under way.

Acknowledgment. This work was supported by the Industrial Technology Research Grant Program in 2003 from the New Energy and Industrial Technology Development Organization (NEDO) of Japan, and the 21st Century COE Program "Nature-Guided Materials Processing". The authors are grateful to Dr. Yoshihiro Ito and Mr. Hiroshi Makino (Kanagawa Academy of Science and Technology) for helpful support in the fluorescence microscopy experiments, and to Dr. Masamichi Kamihira and Mr. Akio Sakaki (Nagoya University) for SPR measurements.

Supporting Information Available. Text giving synthesis of polymer **1**, surface characterizations, and patterning assessments by XPS and fluorescence intensities. This material is available free of charge via the Internet at http://pubs.acs.org.

References and Notes

(1) Ziauddin, J.; Sabatini, D. M. *Nature* **2001**, *411*, 107.
(2) Lange, S. A.; Benes, V.; Kern, D. P.; Höber, J. K. H.; Bernald, A. *Anal. Chem.* **2004**, *76*, 1641.
(3) Yang, Z.; Frey, W.; Oliver, T.; Chilkoti, A. *Langmuir* **2000**, *16*, 1751.
(4) Mrksich, M.; Whitesides, G. M. *Trends Biotechnol.* **1995**, *13*, 228.
(5) (a) Brayan, M. C.; Plettenburg, O.; Sears, P.; Rebuka, D.; Wacowich-Sgarbi, S.; Wong, C.-H. *Chem. Biol.* **2002**, *9*, 713. (b) Fazio, F.; Bryan, M. C.; Blixt, O.; Paulson, J. C.; Wong, C.-H. *J. Am. Chem. Soc.* **2002**, *124*, 14397.
(6) (a) Houseman, B. T.; Mrksich, M. *Chem. Biol.* **2002**, *9*, 443. (b) Su, J.; Mrksich, M. *Angew. Chem., Int. Ed.* **2002**, *41*, 4715.
(7) Park, S.; Shin, I. *Angew. Chem., Int. Ed.* **2002**, *41*, 3180.
(8) Shirahata, N.; Yonezawa, T.; Miura, Y.; Kobayashi, K.; Koumoto, K. *Langmur* **2003**, *19*, 9107.
(9) Tayler, M. E.; Kurt, D. *Introduction to Glycobiology*; Oxford University Press: New York, 2003.
(10) Lee, Y. C. *Carbohydr. Res.* **1978**, *67*, 509.
(11) Ulman, A. *An Introduction to Ultrathin Organic Films: From Langmuir-Blodgett to Self-Assembly*; Academic Press: Boston, MA, 1991.
(12) Lee, Y.-S.; Mrksich, M. *Trends Biotechnol.* **2002**, *20*, 14.
(13) Miura, Y.; Sasao, Y.; Dohi, H.; Nishida, Y.; Kobayashi, K. *Anal. Biochem.* **2002**, *310*, 27.
(14) (a) Sugimura, H.; Hanji, T.; Takai, O.; Masuda, T.; Misawa, H. *Electrochim. Acta* **2001**, *47*, 103. (b) Sugimua, H.; Ushiyama, K.; Hozumi, A.; Takai, O. *Langmuir* **2000**, *16*, 885.
(15) Sugimura, H.; Hozumi, A.; Kameyama, T.; Takai, O. *Adv. Mater.* **2001**, *13*, 667.
(16) (a) Sighavi, R.; Kumar, A.; Lopez, G. P.; Stephanolpoulos, G. N.; Wang, D. I.; Whitesides, G. M.; Ingber, D. E. *Science* **1994**, *264*, 696. (b) Xia, Y.; Mrksich, M.; Kim, E.; Whitesides, G. M. *J. Am. Chem. Soc.* **1995**, *117*, 9576. (c) Aizenberg, J.; Black, A. J.; Whitesides, G. M. *Nature* **1999**, *398*, 495.
(17) Sun, X.-L.; Faucher, K. M.; Houston, M.; Grande, D.; Chaikof, E. L. *J. Am. Chem. Soc.* **2002**, *124*, 7258.
(18) (a) Kobayasi, A.; Akaike, T.; Kobayashi, K.; Sumitomo, H. *Makromol. Chem., Rapid Commun.* **1986**, *7*, 645. (b) Miura, Y.; Ikeda, T.; Kobayashi, K. *Biomacromolecules* **2003**, *4*, 410. (c) Miura, Y.; Ikeda, T.; Wada, N.; Sato, H.; Kobayashi, K. *Green Chem.* **2003**, *5*, 610.
(19) Suzuki, N.; Quesenberry, M. S.; Wang, J. K.; Lee, R. T.; Kobayashi, K.; Lee, Y. C. *Anal. Biochem.* **1997**, *247*, 412.
(20) Scatchard, G. *Ann. N.Y. Acad. Sci.* **1949**, *51*, 660.
(21) (a) Matsuura, K.; Tsuchida, A.; Okahata, Y.; Akaike, T.; Kobayashi, K. *Bull. Chem. Soc. Jpn.* **1998**, *71*, 2973. (b) Tsuchida, A.; Matsuura, K.; Kobayashi, K. *Macromol. Chem. Phys.* **2000**, *201*, 2245.
(22) The adsorption of glycoconjugate polymers was reported in ref 21. In the present case, the thicknesses of the adsorbed layers were evaluated after thorough washing and drying under N_2.
(23) Revell, D. J.; Knight, J. R.; Blyth, D. J.; Haines, A. H.; Russell, D. A. *Langmuir* **1998**, *14*, 4517.
(24) Prime, K. L.; Whitesides, G. M. *Science* **1991**, *252*, 1164.
(25) Luk, Y.-Y.; Kato, M.; Mrksich, M. *Langmuir* **2000**, *16*, 9604.
(26) Hasegwa, T.; Kondoh, S.; Matsuura, K.; Kobayashi, K. *Macromolecules* **1999**, *32*, 6595.
(27) Gestwicki, J. E.; Cairo, C. W.; Strong, L. E.; Octjen, K. A.; Kiessling, L. L. *J. Am. Chem. Soc.* **2002**, *124*, 14922.
(28) Lundquist, J. J.; Toone, E. J. *Chem. Rev.* **2002**, *102*, 555.
(29) Kugumiya, T.; Yagawa, A.; Maeda, A.; Nomoto, H.; Tobe, S.; Kobayashi, K.; Matsuda, T.; Onishi, T.; Akaike, T. *J. Bioactive Biocompatible Polym.* **1992**, *7*, 338.
(30) Lee, C.-S.; Lee, S.-H.; Park, S.-S.; Kim, Y.-K.; Kim, B.-G. *Biosens. Bioelectron.* **2003**, *18*, 437.
(31) Ito, Y.; Nogawa, M.; Sugimura, H.; Takai, O. *Langmuir* **2004**, *20*, 4299.
(32) Mrksich, M.; Whitesides, G. M. *Trends Biotechnol.* **1995**, *13*, 228.
(33) Revzin, A.; Rajagopalan, P.; Tilles, A. W.; Berthiaume, F.; Yarmush, M.; Toner, M. *Langmuir* **2004**, *20*, 2999.
(34) Khademhosseini, A.; Suh, K. Y.; Yang, J. M.; Eng, G.; Yeh, J.; Levenberg, S.; Langer, R. *Biomaterials* **2004**, *25*, 3583.

BM049904T

Available online at www.sciencedirect.com
SCIENCE DIRECT®
Biomaterials 24 (2003) 3511–3519
Biomaterials
www.elsevier.com/locate/biomaterials

Rat costochondral cell characteristics on poly (L-lactide-co-ε-caprolactone) scaffolds

M. Honda[a,b,*], N. Morikawa[c], K. Hata[d], T. Yada[b], S. Morita[c], M. Ueda[a], K. Kimata[b]

[a] *Department of Oral and Maxillofacial Surgery, Postgraduate School of Medicine, Nagoya University, 65 Tsuruma-cho, Showa-ku, Nagoya, Aichi 466-8550, Japan*

[b] *Institute for Molecular Science of Medicine, Aichi Medical University, Nagakute-cho, Aichi-gun, Aichi 480-1195, Japan*

[c] *Division of Research and Development, GUNZE Limited, 1 Ishiburo, Inokura-shinmachi, Ayabe, Kyoto 623-8512, Japan*

[d] *Department of Tissue Engineering, Nagoya University School of Medicine, 65 Tsuruma-cho, Showa-ku, Nagoya, Aichi 466-8550, Japan*

Received 3 October 2002; accepted 24 March 2003

Abstract

This study was designed to examine the adhesion, proliferation, and morphology of chondrocytes on new scaffolds; and to examine these cells histologically for the ability of the chondrocytes to maintain chondrogenic properties after subcutaneous implantation into nude mice. Both 75:25 poly (L-lactide-co-ε-caprolactone) (75PLC) and 50:50 poly (L-lactide-co-ε-capro-lactone) scaffold (50PLC) were tested as a scaffold for rat costochondral resting zone chondrocytes in comparison with a type I collagen sponge scaffold (collagen scaffold). Both of the poly (L-lactide-co-ε-caprolactone) scaffolds (75PLC and 50PLC) were coated with type I collagen solution and the effects of the collagen coat (hybrid-PLC) were also examined. The hybrid-75PLC bound the same number of cells as the collagen scaffold, whereas the 75PLC and the 50PLC bound 60% and 50% fewer cells than the collagen scaffold, respectively. The cell growth on the scaffolds progressed with culture time in all scaffolds. Cell morphology was assessed by scanning electron microscopy for differences in the structure of cellular interaction. Chondrocytes on every scaffold maintained a spherical shape. The hybrid-PLCs were superior to the PLCs with respect to the number of cells attached. The PLCs had an advantageous degradation characteristic in that they retained their original shape better than the collagen scaffold. Additionally, in the PLCs seeded, the cells retained their integrity 4 weeks after implantation, although the volume of collagen scaffold decreased by 50%.

© 2003 Elsevier Science Ltd. All rights reserved.

Keywords: Chondrocytes; Cell ability; Biodegradable polymer scaffold; Poly (L-lactide-co-ε-caprolactone); Hybrid-PLC scaffold; Tissue-engineered cartilage

1. Introduction

Vacanti et al. in 1991 [1] reported the first example of tissue-engineered cartilage using composite grafts of chondrocytes and biodegradable polymer fibers. Over the past decade, scaffolds from natural degradable polymers, such as type I collagen [2], or synthetic degradable polymers, such as polyglycolide (PGA) [3,4], polylactide [5], and copolymers of glycolides with lactides [6] have been extensively investigated for their capability to support the growth of chondrocytes isolated from various animal species [7–9].

Treatment of cartilage repair can be divided into three major areas with quite specific requirements: (1) highly pressure-resistant hyaline cartilage for the repair of traumatic joint defects; (2) genetically modified artificial cartilage to treat defects due to chronic degenerative cartilage disease, such as rheumatoid arthritis; and (3) pre-shaped cartilage replacement for a maxillofacial surgeon to augment defects, e.g., in the nose, outer ear, temporomandibular joint, and temporomandibular disk [10]. In maxillofacial surgery, cartilage grafts have been used to reconstruct auras, nisus, or temporomandibular joint defects resulting from trauma, tumors, or congenital deformities. Currently, autografts, allografts or artificial biomaterials are applied in these situations, and

*Corresponding author. Department of Oral and Maxillofacial Surgery, Postgraduate School of Medicine, Nagoya University, 65 Tsuruma-cho, Showa-ku, Nagoya, Aichi 466-8550, Japan. Tel.: +81-52-744-2348; fax: +81-52-744-2352.

E-mail address: honda-m@naa.att.ne.jp (M. Honda).

0142-9612/03/$ - see front matter © 2003 Elsevier Science Ltd. All rights reserved.
doi:10.1016/S0142-9612(03)00210-2

scaffolds to replace defective cartilage in the craniomaxillofacial region should maintain the original shape for a long term with good strength. The scaffold plays an important role in supporting cell adhesion, growth, and differentiated cell function [11]. The success of tissue-engineered cartilage depends, in part, on the ability of the attachment and the growth of the cells on the scaffold. However, an appropriate synthetic biodegradable polymer scaffold for tissue-engineered cartilage has not yet been established for the maxillofacial region.

We showed that 50:50 poly (L-lactide-ε-caprolactone) scaffold (50PLC) could be used in experimental animals and revealed cartilage tissue formation in vivo [12]. Several reports on the chemical characteristics of poly (L-lactide-co-ε-caprolactone (PLC) have been published [13–15]. PLC in solid form has been used as a biodegradable nerve guide [16], and as an artificial material in cartilage defects. A 50PLC sponge without cells has been used for meniscal reconstruction [17]. At present, PLC as a scaffold for cultured chondrocytes has not been used except for in our study. To select an appropriate scaffold for chondrocytes or determine whether surface modification of the material is needed, it is important to understand how well chondrocytes attach to, and grow on these materials. It is known that collagen type II and poly L-lysine generally improve cell seeding on biodegradable polymers [6].

The aim of this study is to develop a cell-based material engineered in vitro to graft onto the cartilage defects in the maxillofacial region. In this paper, we examined the effects of the attachment, proliferation and morphology of costochondral resting zone chondrocyte seeded on scaffolds including 75:25 poly (L-lactide-ε-caprolactone) (75PLC), 50PLC, 75PLC coated with collagen (hybrid-75PLC), 50PLC coated with collagen (hybrid-50PLC), and a type I collagen scaffold [2,18]. In addition, we also evaluated potentials of these scaffolds for cartilage regeneration.

2. Materials and methods

2.1. Preparations of the biodegradable polymer scaffolds

Five types of the scaffolds were prepared for this study, 75:25 poly (L-lactide-co-ε-caprolactone) (75PLC), 50:50 poly (L-lactide-co-ε-caprolactone) (50PLC), 75PLC coated with collagen (hybrid-75PLC), 50PLC coated with collagen (hybrid-50PLC), and collagen scaffold. The PLCs were prepared as follows. A dioxane solution containing 2.0% (w/w) of PLC was poured into a mold and frozen slowly at −12°C. The frozen content was dried in a freeze drier (FD-520, EYELA, Tokyo, Japan) to yield porous sponge sheets. Sponge sheets were cut 1 mm thick and then into round disks 8 mm in diameter. This procedure was the same as a previously published report [12]. Half of the products were coated with 1.0 mg/ml of type I collagen solution to examine whether it affected chondrocyte attachment to the polymer matrices. After they were kept in a solution for 12 h at 4°C, the matrices were again lyophilized. To cross-link the collagen, hybrid-75PLC was heated at 120°C for 24 h under a vacuum, and the hybrid-50PLC was irradiated under a UV lamp.

Previous collagen scaffold did not reveal cartilage formation when inoculated with primary chondrocytes up to 4 weeks after implantation. This result can be attributed to the 2 weeks degradable period of the collagen scaffold in vivo. To provide the necessary mechanical strength for use in this study, the collagen scaffold was heated at 105°C for 24 h under a vacuum to be cross-linked. Furthermore, the sponge sheet was cross-linked by immersing it in 0.05 M acetic acid containing 0.2% glutaraldehyde at 4°C for 24 h. After washing with distilled water to remove unreacted glutaraldehyde, the sponge sheet was freeze-dried again.

All scaffolds were sterilized by ethylene oxide gas and degassed at 60°C under vacuum for 1 week before each experiment.

These scaffolds were sputter coated with gold and observed under a scanning electron microscope (SEM) (JSM-5800LV, JEOL, Tokyo, Japan) to determine the pore size.

2.2. Cell culture

Chondrocyte culturing in this study was performed essentially as described previously [2,12,19]. All in vitro manipulations were performed in a laminar flow hood using an aseptic technique. Briefly, costochondral cartilage from 4-week-old male Lewis rats was peeled from the fibrous tissue of the cartilage. The resting zone cartilage was separated and cut with surgical scissors into cross-sectionals approximately 3 mm in thickness. These sections were immersed in phosphate-buffered saline (PBS), pH 7.4, without magnesium or calcium ions (PBS (−), Takara Biomedical Pharmaceutical Co., Ltd, Otsu, Japan) containing 0.10% (w/v) ethylenediamine tetraacetic acid (EDTA) twice for 20 min and then PBS (−) containing 0.25% (w/v) trypsin and 0.10% (w/v) EDTA (GIBCO, Grand Island, NY) at 37°C for 1 h. After three washes with PBS (−), the tissues were digested with PBS (+) (GIBCO) containing 0.1% (w/v) collagenase (Wako Pure Chemical Industries, Ltd., Osaka, Japan) at 37°C for 4 h. After washing with PBS (−), the digested cartilage tissues were cultured on plastic dishes (Falcon® Type 3003; Beckton Dickinson & Co., Lincoln Park, NJ). Chondrocytes that migrated from the cartilage tissues were cultured in Dulbecco's Modified Eagle's Medium (DMEM, GIBCO) supple-

mented with 10% (v/v) of fetal calf serum (FCS, GIBCO), penicillin (100 μg/ml), and streptomycin (100 μg/ml) in a humidified atmosphere containing 5% CO_2 at 37°C. The culture medium was replaced every 2 days.

2.3. Cell growth in scaffolds

To assess cell adhesion kinetics, secondarily passaged chondrocytes were seeded onto all the polymer sponges, and kept in a 48-well plate (Becton Dickinson & Co.) at a density of 1.3×10^5 cells/cm^2 (equivalent to approximately 70% confluence). The cells were allowed to attach to the substrates undisturbed in DMEM containing 10% FCS in a humidified incubator (37°C, 5% CO_2) for 2 h, at which time the unattached cells were removed from the substrates with DMEM containing 10% FCS.

At this time point, plates were rinsed gently with PBS (−) and the number of attached cells was quantified by assaying with a tetrazolium salt of 3-(4,5-dimethylthiazol-2-yl)-2,5-diphenyltetrazolium bromide (MTT, Dojindo Laboratories, Kumamoto, Japan) [20].

The attached cells of these scaffolds were allowed to proliferate at 37°C in DMEM containing 10% FCS for 1, 3, 5, and 7 days, at which time the number of attached cells was determined by an MTT assay.

2.4. Evaluation of degradation of scaffolds

All scaffolds used in this study were harvested after implantation periods ranging from 3 weeks to 5 months and evaluated for the rate of degradation. They were cut to the same square areas. A subcutaneous rat model was used to simplify the implantation and evaluation procedures.

The weight of harvested scaffolds were measured and compared to the initial scaffold weight. The fibrous tissue around scaffolds was gently peeled off.

2.5. Scanning electron microscopy

SEM micrographs of chondrocytes that attached to the scaffolds following 8 h of culture (seeding density: 1.3×10^6 cells/cm^2) were taken. Attached chondrocytes were rinsed with a 0.1 M phosphate buffer (pH 7.4). The cells attached to scaffolds were then fixed with 2.5% glutaraldehyde (Wako Pure Chemical Industries, Ltd.) in a 0.1 M phosphate buffer for 2 h. Following three rinses with phosphate buffer, the samples were dehydrated step-wise with ethanol starting at 30% and continuing to 100% for approximately 15 min at each step. Finally, the samples were immersed in *tert*-butanol and freeze-dried, sputter coated with gold, and observed under an SEM (JSM-5800LV, JEOL).

2.6. Fluorescent microscopy

Fluorescent photomicrographs of chondrocytes that attached to scaffolds following 1, 4, and 7 days of culture (seeding density: 1.3×10^6 cells/cm^2) were taken. Attached chondrocytes were rinsed with PBS (−). Scaffolds with attached cells were placed in a solution of the vital dye calcein AM (1 μM, Molecular Probes, Eugene, OR) [21], and the nuclear stain ethidium bromide (0.5 μg/ml, Wako Pure Chemical Industries, Ltd.) in PBS (−). Then scaffolds were incubated at room temperature without agitation for 30 min, and then observed under fluorescent microscopy (BX60, Olympus, Tokyo, Japan) without subsequent washing. Cell viability was indicated by bright green fluorescence in the cytoplasm of the cells. Dead cells were identified by the binding of ethidium bromide to nucleic acids, giving off a bright orange fluorescence.

2.7. Preparation of chondrocyte-scaffold composites and implantation

Chondrocyte-scaffold composites (CSCs) were prepared in an attempt to generate cartilage tissues subcutaneously in nude mice (athymic KSN) as follows. Primarily, cells reached confluence in 21 days. At preconfluence, chondrocytes were treated with PBS (−) containing 0.25% (w/v) trypsin and 0.10% (w/v) EDTA for 15 min. Migrated cells were collected as a chondrocyte suspension (1.0×10^7 cells/ml) in DMEM and inoculated into the hybrid-75PLC (50 mm^2, 2 mm thickness) and the collagen scaffold. All scaffolds were cut to the same area. The CSCs were then incubated in culture medium for 24 h at 37°C before being implanted into the subcutaneous dorsum of 4-week-old male nude mice. Nude mice were anesthetized by intramuscular injection using pentobarbital sodium. A subcutaneous pocket was prepared by blunt dissection on the front sides of the midline incision. The CSCs were placed into the pocket, and the wound was closed in layers with 4-0 Vicryl interrupted sutures. In these groups, we examined 10 specimens for primary chondrocytes, thus determining if the ability of cells to form cartilage was dependent on the scaffold.

2.8. Histological observation

4 weeks after the implantation, the mice were sacrificed and all CSCs were dissected and fixed in 10% buffered formalin for 24 h, dehydrated with graded ethanol and embedded in paraffin. The 5-μm-thick paraffin sections were deparaffinized with xylene, dehydrated and stained with hematoxylin and eosin or alcian blue (pH 1.0) for the presence of sulfated glycosaminoglycans (S-GAGs).

3. Results

3.1. Properties of scaffolds

An SEM of all scaffolds demonstrated a smooth textured surface and regular porous structure (Figs. 1(a–e)). Each scaffold had a similar pore size of 200 μm in diameter.

The remaining mass of the scaffolds was measured and plotted as a function of time, as shown in Fig. 2. After a 3-week implantation, the 75PLC, 50PLC, and collagen scaffold showed mass losses of 83.7%, 53.0%, and 38%, respectively. A difference in mass loss could be observed among the three scaffolds. Although the volume of the 50PLC decreased dramatically after 3 weeks of implantation, that of the 75PLC did so from 12 to 20 weeks. The hybrid-PLCs had a delayed degradation period. The degradation of the collagen scaffold was extremely faster than that of the PLCs.

3.2. Cell proliferation analysis

The number of cells adhering to the scaffolds was measured by MTT assay. Chondrocytes were allowed to attach to the scaffolds up to the initial time point of 2 h (Fig. 3). The greatest number of chondrocytes attached to the hybrid-50PLC, whereas attachment to the 50PLC was much lower than that of other scaffolds. In addition, the cells on the 50PLC did not grow.

For the PLC scaffolds, the collagen treatment led to an increase in the attachment of cells to the scaffold up to 2 h. The 75PLC and the collagen scaffold allowed continued increase in cell number, which was observed throughout the experiments, up to the last time point

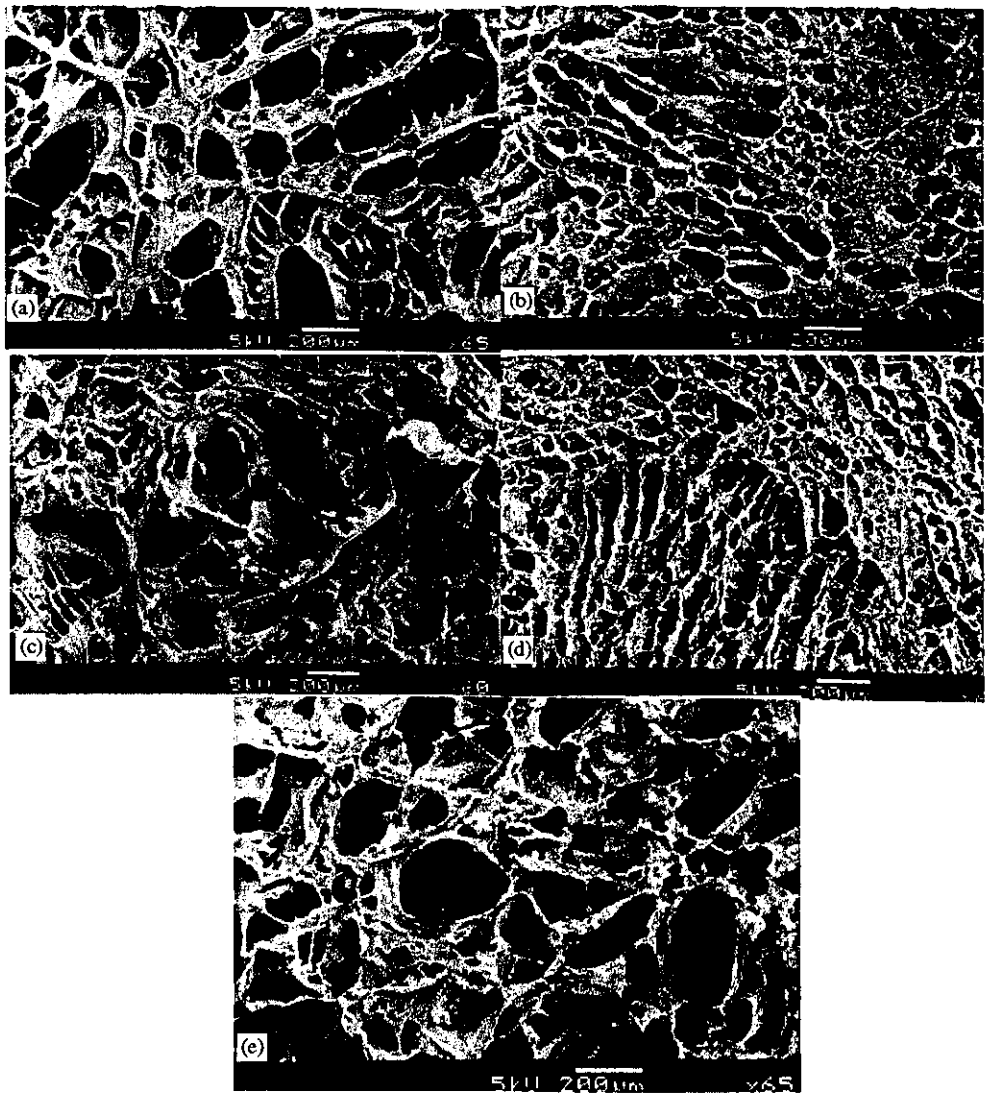

Fig. 1. SEM revealing the rough surfaces of the scaffolds used in this study. ((a) hybrid-75PLC scaffold, (b) 75PLC scaffold, (c) hybrid-50PLC scaffold, (d) 50PLC scaffold, and (e) collagen scaffold).